Journal of
Innate Immunity

Research Article

J Innate Immun 2025;17:154–175
DOI: 10.1159/000543633

Received: September 12, 2024
Accepted: January 13, 2025
Published online: February 27, 2025

Neutrophils Display Novel Partners of Cytosolic Proliferating Cell Nuclear Antigen Involved in Interferon Response in COVID-19 Patients

Lucie Pesenti[a] Rodrigo de Oliveira Formiga[a] Nicola Tamassia[b] Elisa Gardiman[b] François Chable de la Héronnière[a] Sara Gasperini[b] Johana Chicher[c] Lauriane Kuhn[c] Philippe Hammann[c] Morgane Le Gall[a] Giovanni Saraceni-Tasso[a] Clémence Martin[a, d] Anne Hosmalin[a] Magali Breckler[e, f] Roxane Hervé[e, f] Patrice Decker[e, f] Maha Zohra Ladjemi[a] Frédéric Pène[a, g] Pierre-Régis Burgel[a, d] Marco A. Cassatella[b] Véronique Witko-Sarsat[a]

[a]INSERM U1016, Institut Cochin, CNRS 8104, Université Paris Cité, Paris, France; [b]Department of Medicine, Section of General Pathology, University of Verona, Verona, Italy; [c]Strasbourg-Esplanade Proteomics Platform, CNRS UAR1589, Molecular and Cellular Biology Institute, University of Strasbourg, Strasbourg, France; [d]Department of Respiratory Medicine, AP-HP, Cochin Hospital, Paris, France; [e]INSERM UMR 1125, Bobigny, France; [f]UFR SMBH, Li2P, Université Sorbonne Paris Nord, Bobigny, France; [g]Department of Intensive Medicine and Reanimation, AP-HP, Cochin Hospital, Paris, France

Keywords
Neutrophils · Proliferating cell nuclear antigen · Interferon · PAD4 · Histone 3 · COVID-19

Abstract
Introduction: Neutrophils are key players in the hyperinflammatory response during SARS-CoV-2 infection. The cytosolic proliferating cell nuclear antigen (PCNA) is a scaffolding protein highly dependent on the microenvironment status and known to interact with numerous proteins that regulate neutrophil functions. This study aimed to examine the cytosolic protein content and PCNA interactome in neutrophils from COVID-19 patients. ***Methods:*** Proteomic analyses were performed on neutrophil cytosols from healthy donors and patients with severe or critical COVID-19. In vitro approaches were used to explore the biological significance of the COVID-19-specific PCNA interactome. ***Results:*** Neutrophil cytosol analysis revealed a strong interferon (IFN) protein signature, with variations according to disease severity. Interactome analysis identified associations of PCNA with proteins involved in interferon signaling, cytoskeletal organization, and neutrophil extracellular trap (NET) formation, such as protein arginine deiminase type-4 (PADI4) and histone H3, particularly in critical patients. Functional studies of interferon signaling showed that T2AA, a PCNA scaffold inhibitor, downregulated IFN-related genes, including STAT1, MX1, IFIT1, and IFIT2 in

Lucie Pesenti and Rodrigo de Oliveira Formiga contributed equally to this work.

karger@karger.com
www.karger.com/jin

Karger
OPEN ACCESS

Correspondence to:
Véronique Witko-Sarsat, veronique.witko@inserm.fr

neutrophils. Additionally, T2AA specifically inhibited the secretion of CXCL10, an IFN-dependent cytokine. PCNA was also found to interact with key effector proteins implicated in NET formation, such as histone H3, especially in critical COVID-19 cases. ***Conclusion:*** The analysis of the PCNA interactome has unveiled new protein partners that enhance the interferon pathway, thereby modulating immune responses and contributing to hyperinflammation in COVID-19. These findings provide valuable insights into interferon dysregulation in other immune-related conditions.

Introduction

Neutrophils are crucial in host defense and have been recognized for decades for their central role in containing infections [1]. However, this protective function comes with a caveat: when their activation is dysregulated, neutrophils can exacerbate inflammation, releasing highly cytotoxic molecules such as proteases, reactive oxygen species (ROS), cationic proteins, and neutrophil extracellular traps (NETs), often to the detriment of host tissues [2–4]. Consequently, in an inflammatory site, neutrophils have to be cleared in a regulated manner, for instance through apoptosis or enabling activation of pro-resolving circuits, to allow the resolution of inflammation [5, 6]. Harnessing neutrophil functions to stimulate inflammation resolution requires avoiding excessive responses that lead to either hyperinflammation or chronic inflammation, thereby ensuring an immune response tailored to the initial stimulus. Achieving this goal depends on a deeper understanding of the mechanisms that coordinate the multifaceted roles of neutrophils, including survival, activation, migration, and cytokine/chemokine production [7–10].

The proliferating cell nuclear antigen (PCNA) is a scaffolding protein that shapes neutrophils effector mechanisms adapted to a specific inflammatory setting [11, 12]. We have previously described that PCNA is present exclusively within the cytosol in mature neutrophils due to its nuclear export at the end of the granulocytic differentiation [13, 14]. PCNA, originally known as a nuclear protein pivotal in DNA synthesis, replication, and repair, is a key element in controlling neutrophil survival through its association with procaspases to prevent their activation [13]. PCNA regulates the production of ROS via its specific association with cytosolic subunits of the NADPH oxidase but its role is different depending on the state of activation [15]: we have shown that PCNA is associated with the P47phox (within the PX domain) at the resting state to prevent NADPH oxidase activation. However, after stimulation with f-MLF or PMA, this association is disrupted and PCNA migrates to the membrane and presumably through the binding to other components of the NADPH oxidase complex to promote its assembly. Accordingly, disrupting the PCNA scaffold using either a competing P21 peptide [13] or a small molecule T2AA has a strong inhibitory effect on NADPH oxidase-dependent ROS production [15]. T2AA, a cell-permeable inhibitor, disrupts PCNA/PIP-box interactions and binds specifically to PCNA at the PIP-box cavity and an adjacent site near Lys-164 on the PCNA homotrimer interface. These properties confer high specificity, including an affinity for monoubiquitinated PCNA, although potential off-target effects cannot be fully excluded [16]. Given the essential role of PCNA in cell viability, genetic knockout models are unavailable, making T2AA an invaluable tool for probing PCNA-dependent pathways. Interestingly, the strong induction of cytosolic PCNA upon G-CSF treatment and the profound reorganization of its scaffold suggest that PCNA may be a key orchestrator of neutrophil functions in response to an inflammatory stimulus [16–18]. G-CSF is critical to neutrophil granulopoiesis and modulates the functions and the metabolism of neutrophils through its “switch effect” on PCNA scaffold. Accordingly, we have identified protein partners that were either released from or newly associated to PCNA in neutrophils from G-CSF-treated donors, suggesting that PCNA scaffold is extremely plastic reprogramming neutrophils toward distinct repertoire adapted to the inflammatory setting [17]. In addition, PCNA can associate with the nicotinamide phosphoribosyltransferase to promote NAD^+ synthesis that controls energy metabolism [19]. This PCNA-nicotinamide phosphoribosyltransferase interaction is also prominent in chemotherapy-resistant leukemic myeloid cells, underscoring its role in stress and inflammatory conditions [19]. At rest, cytosolic PCNA acts as a gatekeeper, maintaining neutrophil integrity and preventing inappropriate activation. In contrast, under inflammatory stress, PCNA facilitates NADPH oxidase assembly and coordinates various effector functions, including metabolic rewiring, to adapt neutrophil responses to pathological conditions.

The recent COVID-19 pandemic caused by the novel coronavirus SARS-CoV-2 represents an example in which neutrophils emerge as central players in host defense [20], but also for the onset, disease establishment and even in post recovery phase if their response is not properly regulated [21–23]. Neutrophils-related mediators, such as the NETs, web-like structures composed of DNA-histone or mitochondrial DNA complexes expulsed extracellularly along with cytosolic antimicrobial proteins [24, 25], were found to be enhanced in the circulation and lungs of patients leading to microvascular thrombosis, including in patients displaying the acute respiratory distress syndrome (ARDS). Such molecules were associated throughout the pandemics as a marker of disease severity and poor prognosis [26–31].

For instance, in the most serious COVID-19 cases, an apparent impaired IFN-α and -β signaling is related to blood viral load persistency and to high proinflammatory activity, perhaps linked to a skewed stimulation of subpopulations of plasmacytoid dendritic cells (pDC) that stimulate an excess of inflammatory mediators [32–34]. On the other hand, IFN-γ displays a high association with immune markers of poor prognosis, such as the C-reactive protein and a high number of positive associations with CXCL8, IL-1ra, TNF-α, and CXCL10 [35]. Numerous studies have shown that patients with severe COVID-19 frequently exhibit a dysregulated IFN response. This can manifest as insufficient IFN levels, resulting in poor antiviral defense, or as an imbalanced response that drives excessive inflammation [36, 37]. The dynamics of type I IFNs in severe cases align with observations from murine models of SARS-CoV-2 infection, which demonstrate that type I IFNs are ineffective at controlling viral replication in vivo but contribute to pathological responses [38]. Furthermore, some severe COVID-19 patients develop autoantibodies against various IFN subtypes, effectively neutralizing their antiviral effects, even when IFN responses are otherwise normal [34, 39].

The complexity of this dysregulation stems from two key factors. First, the specific IFN subtype: while subtypes such as IFNA2 and IFNG are associated with strong antiviral activity, others, like IFNB1 and IFNA6, are linked to endothelial damage and platelet activation [35]. Second, the diversity of IFN-producing cells adds another layer of complexity. IFNs coordinate the immune response by activating and recruiting various immune cells, including macrophages, dendritic cells, and T cells. Disruptions in this IFN signaling cascade often result in the imbalanced immune responses observed in severe COVID-19 patients [37]. Notably, the role of neutrophils in the IFN signaling relay and their potential contribution to IFN dysregulation remains to be fully determined. Even though neutrophils do not normally produce large amounts of IFN, they are responsive to IFN-mediated signaling [40–43], and most importantly in COVID-19 patients exhibit elevated levels of IFN-stimulated genes (ISGs) in those cells, correlating with disease severity [44, 45]. Nevertheless, the proteome of neutrophils studied longitudinally from individuals hospitalized with different stages of COVID-19 demonstrated an initial upregulation of the IFN pathway, but this signature rapidly declined in patients with severe disease, suggesting the presence of circulating cells showing distinct proteomes with metabolic alterations and immunosuppressive profiles [46]. How neutrophils are shaped during inflammation as well as the molecular mechanisms favoring their dysregulation is yet to be determined and holds promise for future host-directed interventions, which could mitigate excessive immune responses, reduce tissue damage, and improve outcomes in inflammatory diseases, such as COVID-19. This study aims to unravel the pathological PCNA scaffold in COVID-19, shedding light on the diverse PCNA-dependent regulatory pathways governing neutrophil activation during the disease.

Patients and Methods

Human Blood Samples

Individuals hospitalized due to COVID-19 from April 2020 to January 2022 were recruited at the Pneumology Department and Intensive Care Medicine Unite from Cochin Hospital in Paris, France. Each patient was classified into different clinical severity groups. Severe patients require COVID-19 oxygen flow between or over 3 L/min. Critically ill patients require more than 60% high-flow oxygen and ventilation and have been admitted to the Intensive Care Unit (ICU). Patient classification is reported in Table 1 based on the patients' oxygen needs and overall clinical state. Blood samples from COVID-19 patients and from healthy donors (HDs) obtained from the *Etablissement Francais du Sang* were collected in EDTA-vacuum tubes.

Neutrophil Isolation and Cytosolic Fraction Recovery

Neutrophils were isolated by LPS-free dextran sedimentation and Ficoll (Histopaque-1077®, Sigma-Aldrich) centrifugation, as previously described [13]. Briefly, whole blood was layered onto Ficoll-Histopaque (Density 1.077 g/mL, Sigma-Aldrich) and centrifuged at 700 *g* for 30 min. The red blood cells and neutrophils were resuspended in Dextran 2% diluted in NaCl 0.9% (Sigma-Aldrich). Sedimentation time was 50 min. The supernatant containing the neutrophils was collected

Table 1. Demographical and clinical characteristics of COVID-19 patients included in the study

	COVID-19	
	severe	critical
Male sex, *n*	5	6
Female sex, *n*	2	1
Age, median (IQR), years[a]	80.3 (72–92)	71.4 (62–78)
Prior comorbid conditions		
Hypertension	4	5
Diabetes	2	3
Obesity (BMI >30 kg/m^2)	2	3
Leukocytes, /μL[b]	7,012±967.6	9,607±1,256
Neutrophils, /μL[b]	5,149±1,003	7,947±1,055
CRP, mg/dL[b]	94.9±29.7	123.9
Noninvasive oxygen support	7	7
Oxygen flow <3 L/min, *n*	2	0
Oxygen flow >3 L/min, *n*	3	7
Nasal high flow oxygen, *n*	4	7
Invasive mechanical ventilation	0	6
Systemic corticosteroid therapy during hospitalization	7	7
Complete hospitalization duration, median (IQR), days	26.3 (15–72)	31.25 (9–52)

IQR, interquartile range. [a]Results are expressed as median (min-max values). [b]Results are expressed as mean ± SEM.

and centrifuged at 500 *g* for 5 min. The supernatant was discarded and the remaining red blood cells were lysed in NaCl 0.2% for 40 s, and then NaCl 1.6% was added. The sample was centrifuged for 5 min at 500 *g* and the procedure of lysis was repeated for another 2–3 times until a white pellet was obtained. Thereafter, the pellet was resuspended in complete culture medium consisting in RPMI 1640 medium with GlutaMAX (Gibco) supplemented with 10% heat-inactivated fetal bovine serum (FBS), 100 units/mL penicillin and 100 μg/mL streptomycin mix (Gibco), and 10 mM HEPES (Gibco) to be counted and used for experiments. In specific experiments for mRNA expression and cytokine production, isolation of neutrophils was performed by the EasySep Neutrophil Enrichment Kit (StemCell Technologies), to reach an approximately 99.7% cell purity. The neutrophil cytosolic fraction was obtained by sonication in a hypotonic buffer as previously described [47]. Briefly, neutrophils were suspended at 100×10^6 cells/mL in a HEPES buffer (50 mM) supplemented with protease inhibitors (4 mM PMSF, 400 μM leupeptin, 400 μM pepstatin, 1 mM orthovanadate, 1 mM EGTA, and 1 mM EDTA) and DTT (1 mM), with a Soniprep 150 Plus sonicator (1 Hz for 10 s). After centrifugation for 15 min at 10,000 *g* at 4°C, the supernatant was collected and stored at −80°C for further analysis.

Proteomic Analysis

Differential proteomic analysis (HD n = 4; severe COVID-19 n = 4; critical COVID-19 n = 4) was carried out on neutrophil cytosols. For basal cytosolic analyses, 10 μg of Bradford quantified proteins were precipitated with methanol before being digested with sequencing-grade trypsin (1:30, Promega, Fitchburg, MA, USA). Each sample was analyzed by nanoLC-MS/MS on a QExactive+ mass spectrometer coupled to an EASY-nanoLC-1000 (Thermo Fisher Scientific, USA) as described previously [48]. Data were searched against the SwissProt Human database (v2021-02) with a decoy strategy. Peptides and proteins were identified with the Mascot algorithm (version 2.6, Matrix Science, London, UK) and data were imported into Proline v2.0 software [49]. Proteins were validated on Mascot pretty rank equal to 1, a Mascot score threshold set at 25 and 1% false discovery rate on both peptide spectrum matches (PSM score) and protein sets (Protein Set score). The total number of MS/

MS fragmentation spectra was used to quantify each protein in 4 patients from all the conditions (controls and coIPs) with the *R* package IPinquiry [50]. After a DEseq2 normalization of the data matrix, the spectral count values were submitted to a negative binomial test using an edgeR GLM regression through R (R v4.0.3). For each identified protein, an adjusted p value (adjp) corrected by Benjamini-Hochberg was calculated, as well as a protein fold change. The results are presented in a Volcano plot using protein log2 fold changes and their corresponding adjusted *p* value (-log10adjp) to highlight enriched and depleted proteins.

Statistical overrepresentation reactome pathways were identified by the software Panther 19.0 using a right-tailed Fisher's exact test with a Bonferroni correction (significance level *p* value <0.05). Functional analysis was also performed using the software Ingenuity 24.0 to identify statistically modulated pathways. Proteins were considered differentially expressed (DE) when the log fold change was superior to 1 and with an adjusted $p < 0.05$.

Interactome Evaluation by Mass Spectrometry

Interactomic analyses (HD = 2; severe COVID-19 $n = 2$; critical COVID-19 $n = 2$) were performed as previously described with slight modifications [15] according to the manufacturer's instructions. PCNA was immunoprecipitated in the cytosol of neutrophils (either from HD or from COVID-19 patients) using a rabbit polyclonal anti-PCNA (Ab5). Briefly, 500 µg of lysed proteins were incubated with 2 µg of antibody and 50 µL of protein G Miltenyi magnetic beads. After several washes, proteins were eluted with 95°C elution buffer and proteins were prepared for mass spectrometry analyses as above to be injected with 160-min gradients on the QExactive+ mass spectrometer.

Analysis of Gene Expression

Ultrapure HD neutrophils were suspended at 5×10^6 cells/mL in RPMI 1640 medium supplemented with 10% low-endotoxin FBS (<0.5 EU/mL endotoxin, Sigma-Aldrich), treated with or without 1,000 U/mL pegylated IFNα-2a (Pegasys, Roche), 200 U/mL IFN-γ (R&D Systems, Minneapolis, MN, USA), 10 ng/mL TNF-α (R&D Systems), or 10 µM T2-amine alcohol (T2AA), a PCNA inhibitor, and then plated into 48-well tissue culture plates (from Greiner Bio-One) for culture at 37°C, 5% CO_2 atmosphere. After the desired incubation period (see the Results section), ultrapure HD neutrophils were pelleted by centrifugation and then total RNA was extracted by RNeasy mini kit (Qiagen). To completely remove any possible contaminating DNA, an on-column DNase digestion with the RNase-free DNase set (QIAGEN) was performed during total RNA isolation. Reverse-transcription quantitative real-time PCR (RT-qPCR) was performed essentially as already reported [51]. Purified RNA was reverse-transcribed into cDNA using PrimeScript™ RT Reagent kit (Takara, Japan), while qPCR was carried out using TB Green® Premix Ex Taq™ (Takara). Sequences of gene-specific primer pairs (Life Technologies) are listed in Table 2. Data were calculated by Q-Gene software (https://www.gene-quantification.de/download.html) and expressed as mean normalized expression units after GAPDH normalization.

Assessment of Cytokine Production

After the desired incubation period (see the Results section), ultrapure HD neutrophils were collected and spun at 300 g for 5 min. Cell-free supernatants were collected and immediately frozen and stored at −80°C. Cytokine concentrations in cell-free supernatants were measured by commercially available ELISA kits, specific for human CXCL10 and BAFF (R&D systems). The lowest detection limits of these ELISA were 31.2 pg/mL for CXCL10 and 39.1 pg/mL for BAFF.

NET Induction and Measurement

Freshly isolated HD neutrophils were seeded onto poly-L-lysine-coated (0.001%, Sigma-Aldrich) chamber slides, allowed to settle for 30 min, and stimulated with 8 µM ionomycin in RPMI 1640 medium supplemented with 10% FBS. After 4 h, supernatants were discarded, and NETs were fixed with 4% paraformaldehyde and washed. Chamber slides were blocked using a solution containing 2% bovine serum albumin (Sigma-Aldrich), 2% heat-inactivated goat serum (Eurobio), and 0.2% Triton X-100 (Sigma-Aldrich). NETs were then stained with an anti-histone monoclonal antibody (clone H11-4, pan histones, Millipore) and an anti-neutrophil elastase rabbit polyclonal antibody (Abcam), followed by incubation with AlexaFluor647-conjugated goat anti-mouse IgG and AlexaFluor546-conjugated goat anti-rabbit IgG secondary antibodies (Life Technologies). After washing, NETs were counterstained with Sytox Green DNA dye (Life Technologies) and analyzed using a Zeiss Axio Observer fluorescence microscope.

For live imaging of NET formation, freshly isolated HD neutrophils were stained with 1 µg/mL Hoechst 33342 (Invitrogen) for 30 min at 37°C. Neutrophils were seeded onto poly-L-lysine-coated (0.001%) chambered µ-slides (Ibidi), allowed to settle for 30 min, preincubated with or without 25 µM T2AA for 1 h, and stimulated with

Table 2. Sequences of specific primer pairs for human genes used in RT-qPCR experiments

Gene	Forward primers	Reverse primers
GAPDH	AACAGCCTCAAGATCATCAGC	GGATGATGTTCTGGAGAGCC
STAT1	ACAAGGTGGCAGGATGTCTC	GAAAACGGATGGTGGCAAATG
IFIT1	TCATCAGGTCAAGGATAGTCTG	GGTGTTTCACATAGGCTAGTAG
IFIT2	ACTGCAACCATGAGTGAGAAC	GCCTCGTTTTGCCCTTTGAG
MX1	CTGTAAATCTCTGCCCCTGTTAG	TCGTGTCGGAGTCTGGTAAAC

8 µM ionomycin in RPMI 1640 medium supplemented with 10% FBS. Extracellular DNA was stained with Sytox Green DNA dye (Life Technologies). Imaging was performed on a Zeiss Axio Observer fluorescence microscope using VisiView software (Visitron) at 37°C for 5 h. Images were acquired every 3 min using DAPI and FITC filters. Quantification of FITC fluorescence surface area was carried out using Histolab software (Microvision).

For soluble NET quantification, freshly isolated HD neutrophils were seeded onto poly-L-lysine-coated (0.001%) borosilicate chamber slides (NUNC), allowed to settle for 30 min, preincubated with or without 25 µM T2AA for 1 h, and activated with 4–8 µM ionomycin in RPMI 1640 medium without FBS. After 4 h, the chambers were washed twice with PBS (Thermo Fisher), and NETs were detached from the glass by gentle digestion with deoxyribonuclease 1 (Sigma-Aldrich). The reaction was stopped by adding 3 mM EDTA. Supernatants containing soluble NETs were collected and centrifuged at 300 *g* for 10 min to remove intact cells. The upper phase was collected and centrifuged again at 16,000 *g* for 10 min to remove cell debris, and the final supernatant was collected and frozen. Soluble NETs were quantified using PicoGreen dye, a fluorescent probe for double-stranded DNA (Life Technologies), as previously described [52].

Immunofluorescence Labeling and Duolink Proximity Ligation Assay

When indicated, neutrophils from HD or from COVID-19 patients were resuspended at 2×10^6 cells/mL and were incubated in RPMI medium containing 10% fetal calf serum for the indicated time at 37C° and 5% CO_2. Neutrophils were deposited on a slide to adhere for 15 min at 37°C and were left untreated or were treated with IFN-α (Preprotech, 100 ng/mL), or IFN-γ (Preprotech, 25 ng/mL) in the absence or in the presence of ionomycin (4 µM) or T2AA (10 µM). After the incubation, neutrophils were fixed with 4% formaldehyde (Sigma-Aldrich) for 20 min on ice and kept at 4°C. Cells were permeabilized with Triton X-100 (0.25%) for 10 min at RT and blocked with PBS 5% BSA for 2 h at RT. Then, cells were incubated at 4°C with primary antibodies either rabbit-monoclonal antibody anti-phosphorylated-STAT1 (p-STAT1) (Cell signaling, clone 58D6 diluted 1:100) or mouse anti-PCNA (Abbkine; 1:100) or histone-H3 (Abcam; 1:500) or citrullinated H3 (Cit-H3) (Abcam; 1:500) diluted in PBS 1% BSA, overnight followed by fluorochrome-coupled secondary antibodies as appropriate either goat-anti-rabbit STAR 580 (Abberior) or goat-anti-mouse Alexa Fluor 488 (Invitrogen) diluted 1:1,000 in PBS 1% BSA for 1 h. Nuclei were stained with Hoechst 33342 solution (diluted 1:6,000 in PBS) for 10 min. Slides were mounted using Fluoromount-GTM medium (Invitrogen). Image acquisitions were performed at the Cochin Institute Imaging Facility (IMAG'IC, INSERM U1016, Paris, France) using Widefield Zeiss Observer Z1 or IXplore spinning confocal. Imaging of anti-mouse Alexa Fluor 488, anti-rabbit Abberior STAR 580 and Hoechst was obtained using the multitrack mode. Digital pictures were analyzed and quantified using FIJI software (Version 2.14.0/1,54j).

For the Duolink® proximity ligation assay (PLA), neutrophils (0.3×10^6) were fixed in PBS containing 4% formaldehyde (Sigma-Aldrich) for 20 min on ice and were next cytospined (300,000 cells) in SuperFrost slides to perform immunofluorescence according to manufacturer's instructions. Cells were permeabilized with 0.25% Triton X-100 and were processed as described by the manufacturer using a mix of either mouse anti-PCNA (Abbkine; 1:100) or rabbit anti-PCNA (Invitrogen; 1:100) and anti-PADI4 (Abcam; 1:250), H3 (Abcam; 1:500), or Cit-H3 (Abcam; 1:500) or p-STAT1 (Cell Signaling, clone 58D6 diluted 1:100) as primary antibodies. Detection was achieved if the distance between the two targeted epitopes is up to 40 nm. Fluorescence was acquired under microscopy (Widefield Zeiss Observer Z1). The fluorescent images were then analyzed and quantified using FIJI software (Version 2.14.0/1,54j) by selecting one cell at a time in an image and measuring the area, integrated density, and mean gray value. Using the calculation for corrected total cell fluorescence = integrated density − (area of selected cell × mean fluorescence of background readings). For each image, three background areas were used to normalize against autofluorescence. For each condition, 3–7 images were acquired so that many cells per donor and per condition were available for analysis.

Statistical Analysis

Statistical analyses and graphs were performed with Prism version 10 (GraphPad Software, San Diego, USA). For proteomic analysis, a right-tailed Fisher's exact test with a Bonferroni correction (significance level $p < 0.05$) was performed. To compare two populations for the analysis of fluorescence quantification, a Mann-Whitney test was used for unpaired data or a Wilcoxon test for paired data. A Kruskal-Wallis test with Dunn's post hoc analysis was performed to compare more than two unpaired groups. When indicated, a two-way ANOVA with Sidak's multiple-comparison test was used. Differences were considered significant when $p < 0.05$. Statistical differences between groups were calculated using the appropriate test as indicated. A $p < 0.05$ was considered significant.

Results

Neutrophil cytosolic protein composition is altered in COVID-19 patients with a more profound dysregulation in critical compared to severe patients. Several studies have investigated circulating neutrophils isolated from patients during the course of COVID-19 [45, 46, 53, 54], mostly using whole cell lysates that include proteins from nuclei, membranes, and all types of granules. In this study, we used a proteomic approach to compare the cytosolic fraction of neutrophils obtained by sonication from HDs ($n = 4$) and from COVID-19 patients with varying clinical characteristics, including severe patients admitted to the Pneumology Department (severe, $n = 4$) and critical COVID-19 patients hospitalized in the ICU (critical, $n = 4$) as described in Table 1. For the initial proteomic analysis, the mean ± SEM age was as follows: healthy controls: 52 ± 7.1 years; severe COVID-19: 82.5 ± 6.6 years; and critical COVID-19: 73.5 ± 5.1 years ($n = 4$ for each group). Principal component analysis (PCA) revealed distinct proteomic profiles among the three assessed groups (Fig. 1a). Despite the heterogeneity among COVID-19 patients due to their age that is indicated on the PCA, and their comorbidities (see Table 1), the PCA shows a clear grouping of COVID-19 samples. This suggests that the dysregulation in the cytosolic proteome in COVID-19 patients was so pronounced that the effects of initial conditions, such as age or comorbidities, were less prominent in defining the proteomic signature of COVID-19. The expression pattern of statistically DE proteins was visualized as a heat map, using unsupervised hierarchical clustering indicating relative protein levels detected in each subject (columns) for all biomarkers tested (rows) (Fig. 1b). An increase in the number of detected cytosolic proteins was observed in neutrophils from severe (808 proteins) and critical (860 proteins) COVID-19 patients compared to HD (582 proteins) (online suppl. Fig. S1a; for all online suppl. material, see https://doi.org/10.1159/000543633). We identified 141 proteins DE between HD and severe COVID-19 patients, and 122 proteins between HD and critical COVID-19 patients (online suppl. Fig. S1b, S1c). Totally 78 DE proteins were common between severe and critical COVID-19 patients, with a cutoff at $p < 0.05$ and a fold change >1.5. Pathway enrichment analysis of the DE proteins, using QIAGEN Interacting Pathway Analysis, identified molecular and cellular functions altered in neutrophils from HD versus COVID-19 (Fig. 1c). Consistent with previous studies, we observed that DE proteins in COVID-19 patients were associated with immune activation and with the IFN pathway. Conversely, except for the interferon (IFN) signaling pathway which is prominent in this signature, similar pathways were found to be downregulated since any pathway contains both inhibitory and activating proteins (online suppl. Fig. S2). Using immunofluorescence labeling, we first confirmed that isolated neutrophils from COVID-19 patients have a constitutive expression of p-STAT1, thereby providing evidence that the response pathway to either IFN-α or IFN-γ may be activated in vivo in circulating neutrophils. In contrast, p-STAT1 was not detected in untreated neutrophils from HD, but required an in vitro treatment with IFN-α to be detected as shown in the representative experiment (Fig. 1d). Accordingly, the fluorescence quantification showed a significant increase in p-STAT1 in interferon-treated compared to IFN-untreated neutrophils from HD ($p < 0.001$). Pertinently, we observed that the fluorescence of p-STAT1 in resting neutrophils from COVID-19 patients was even higher than those in interferon-treated HD neutrophils (Fig. 1e) ($p < 0.05$).

Next, we examined the differential proteomic profiles between the severe and critical patient groups. A complete list of the cytosolic proteins that are differentially regulated in neutrophils from COVID-19 patients is provided online in online supplementary Tables S1 and

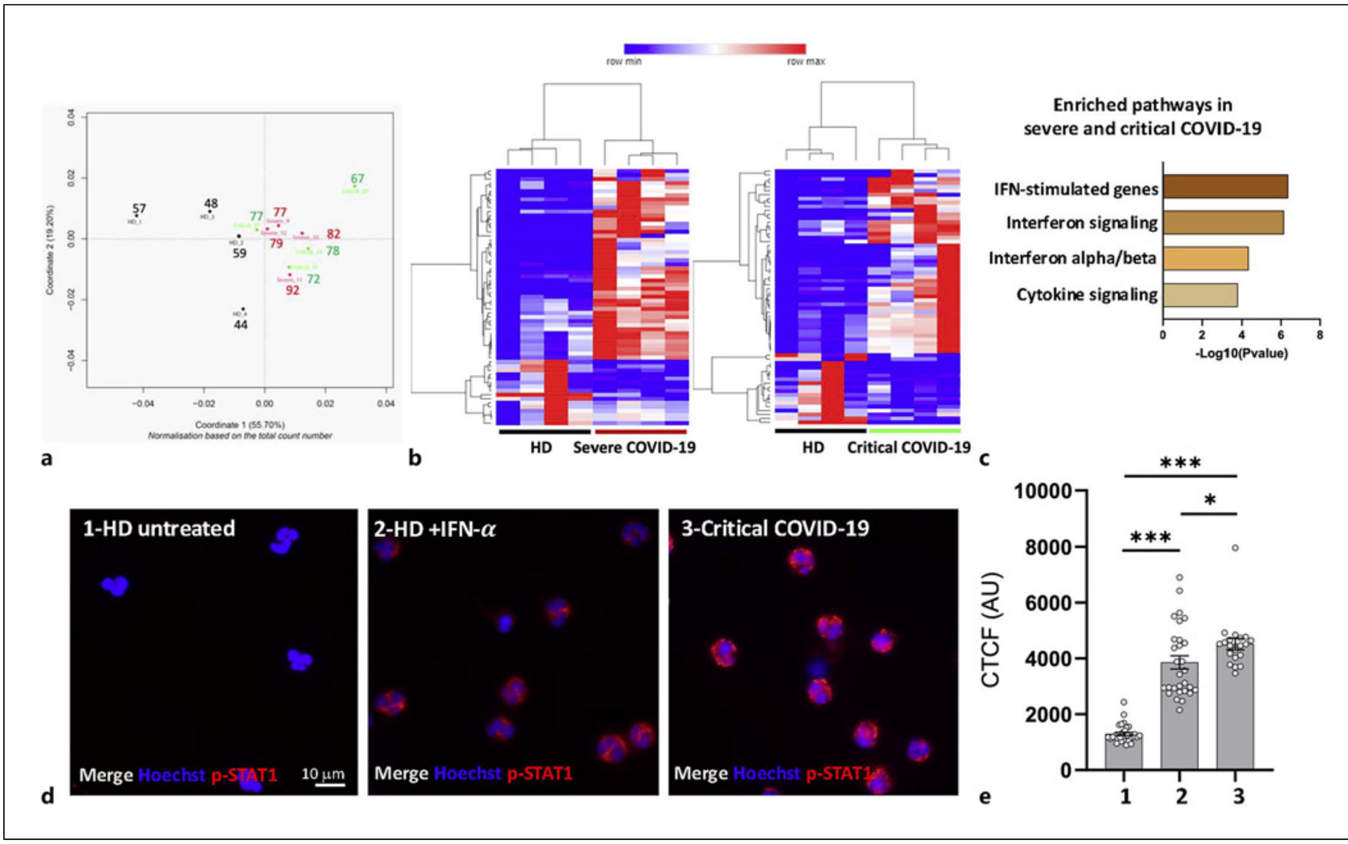

Fig. 1. Proteomic analysis of neutrophil cytosol in HD compared to patients with COVID-19. **a** PCA of the 3 groups of samples: HDs (black; $n = 4$); severe COVID-19 patients (green, $n = 4$); and critical COVID-19 patients (red, $n = 4$). The age of each individual is indicated. **b** Heat map showing the clustering of proteins in the COVID-19 samples versus HD. Data are Z-scored and normalized. **c** Pathway enrichment analyzed using the PANTHER software in the two groups of COVID-19 patients versus HD. **d**, **e** Immunofluorescence labeling of p-STAT1 on isolated neutrophils from critical COVID-19 patients ($n = 2$) and from HD treated or not with IFN-α ($n = 3$). **d** Representative experiment showing the cytosolic fluorescence of p-STAT1. This experiment has been performed with neutrophils from three different HDs and with two different COVID-19 patients. **e** Quantification of the intensity of the cellular fluorescence observed in **d** was performed as described in the Materials and Methods section. Data are means of corrected fluorescence/cell ± SEM. Statistical analysis has been performed using the nonparametric Mann-Whitney test. $^{**}p < 0.01$.

S2. Enriched pathway analysis provided evidence of pathways involved in cell activation (metabolism of proteins, protein kinase R pathway indicative of an interferon-induced kinase that plays a key role in the innate immunity, modulation of G-CSF signaling) in neutrophil cytosol from severe COVID-19 patients (Fig. 2a, b), whereas pathways involved in immune dysregulation (cytokine signaling and peptide loading on class I MHC) were overrepresented in critical patients (Fig. 2c, d). Analysis of proteins enriched in the cytosol from COVID-19 patients showed a common pattern of disturbance in regulatory proteins, including IFN-related proteins (MX1, MX2, IFIT2, IFIT3, OAS3, GBP1), chaperone proteins involved in protein secretion (endoplasmin, ENPL, ENPLL), the phosphorylation/activation of STAT1 (HSP90B), endoplasmic reticulum chaperones such as BIP and calreticulin (CALR), the peptidyl-prolyl cis-trans isomerase with co-chaperone activities (FKBP5), and the GTP-binding protein and Ras-related protein (Rab-44). Additionally, in neutrophils from COVID-19 patients, regardless of disease severity, cytosolic enzymes involved in metabolism regulation were modulated. For instance, the polyunsaturated fatty acid lipoxygenase (LOX15) involved in lipid peroxidation was decreased, suggesting a potential effect on pro-resolving lipids synthesis that remains to be characterized. Of particular interest were the glucose metabolism-associated proteins since they have a specific impact on neutrophil energetic balance, presumably impacting their effector mechanisms (online suppl. Fig. S3, S4). We

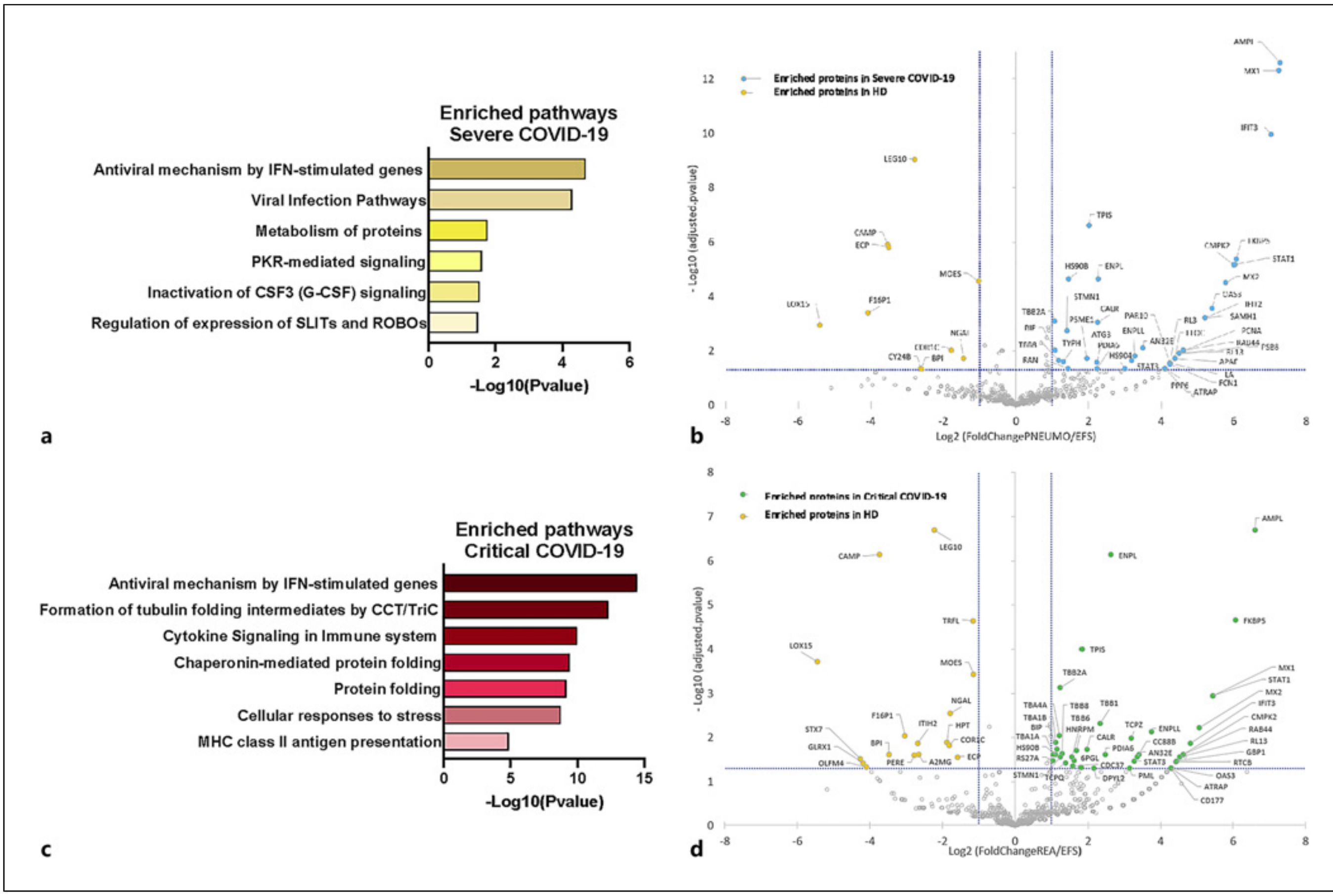

Fig. 2. DE proteins identified in cytosols from COVID-19 patients. Quantitative comparison of DE proteins in controls ($n = 4$) versus severe COVID-19 patients ($n = 4$) (**a**, **b**) and versus critical COVID-19 patients ($n = 4$) (**c**, **d**). Signaling pathways enrichment in neutrophil cytosols that are differentially regulated in severe patients (**a**) (in yellow) and in critical patients (**c**) (in red) versus HD have been analyzed using the PANTHER software. The volcano plot represents relative protein expression changes between COVID-19 patients and HD. Blue and green dots indicate proteins upregulated in COVID-19 in severe and critical, respectively, versus HD with a multicomparison adjusted −log10 (p value) ≥1.3 and a Log2(fold change) ≥1; yellow dots indicate proteins downregulated in COVID-19 versus HD with a multicomparison adjusted −log10 (p value) ≥1.3 and a Log2(fold change) <−1; gray dots indicate proteins that do not meet either criterion.

herein observed that proteins differentially regulated in glycolysis, namely 6-phosphofructo-2-kinase (F262) and triosephosphate isomerase, are significantly increased in both severe and critical COVID-19 versus HD samples (online suppl. Fig. S5). In contrast, we observed a downregulation in the enzyme fructose 1,6-bisphosphatase 1, a rate-limiting enzyme in gluconeogenesis, that is involved in gluconeogenesis in both severe and critical COVID-19 versus HD samples (online suppl. Fig. S6). Contrasting modulation in glycogen synthase (GYS1) enrichment was observed between severe (upregulation) and critical (not statistically significant downregulation) COVID-19 samples versus HD (online suppl. Fig. S7). Finally, we observed a significant enrichment in the glucose-6-phosphate1-dehydrogenase, which is the initial enzyme for the pentose phosphate shunt, both in severe and in critical COVID-19 samples versus HD suggesting an upregulation of this pathway (online suppl. Fig. S8). Taking together, we confirm a global dysregulation in the glucose metabolism-associated proteins, which might impact the global energy metabolism of neutrophils.

Cytosolic PCNA Interacts with Different Protein Partners in Neutrophils from COVID-19 Patients

Since PCNA protein levels may be affected under distinct conditions [13, 17], we first examined their abundance in neutrophils from COVID-19 patients by analyzing publicly available data from previous proteomic studies [45, 46, 53]. Notably, PCNA amounts were found to be significantly upregulated in different datasets obtained in a global proteomic analysis COVID-19 and HD neutrophils were compared (online suppl. Fig. S9). Specifically in the dataset from Kaiser et al. [53], the PCNA levels were enhanced in the most debilitated patients, suggesting the association with disease severity (online suppl. Fig. S9a). Importantly, using immunofluorescence labeling, we provide evidence that PCNA localization was exclusively cytosolic in both HD and COVID-19, confirmed higher intensity levels correlated with severity (online suppl. Fig. S9b). Notably, taking neutrophils from G-CSF-treated donors as an example, we previously provided strong evidence on how immune activation robustly increased PCNA amounts, but also triggered a clear reconstruction of a new scaffold adapted to the inflammatory context [17]. Therefore, to dissect the molecular scaffold of cytosolic PCNA in COVID-19, we performed a coimmunoprecipitation of PCNA from neutrophil cytosol followed by mass spectrometry identification of partner proteins. More proteins were bound to PCNA in COVID-19 compared to HDs, presumably due to the high levels of PCNA expression, as illustrated by the volcano plots representation for severe (Fig. 3a) and ICU (Fig. 3b) COVID-19 patients. A different profile of interacting proteins was observed in severe COVID-19 patients versus critical COVID-19 patients with a total of 56 and 66 proteins identified in severe versus critical, respectively, and 41 common partner proteins (online suppl. Tables S3, S4). Interacting pathway analysis uncovered differences in PCNA interactors in cytosols from severe (Fig. 4a) or critical cases (Fig. 4b) compared to HD, as illustrated by string representation. In neutrophils from either severe or critical patients, cytosolic PCNA was associated with proteins belonging to the IFN signaling pathway, including MX1, MX2, OAS3, and CMPK2. On the other hand, STAT1 was also shown to be linked to PCNA, but exclusively in critical patients. PCNA was also associated with cytoskeleton proteins in COVID-19, such as tubulin, and with proteins involved in NET formation, notably the peptidyl arginine deiminase type 4 (PADI4) and the histone H3. In contrast to PADI4 that was detected to interact with PCNA in both disease groups, histone H3 was assessed only in critical patients (Fig. 3, 4a, b), suggesting that this pathway was differentially mobilized in the most serious COVID-19 cases. Of note, the new hit partners identified in the PCNA interactome in COVID-19 patients, namely IFN-related proteins and PAD4 and histone 3, were not present in the neutrophil PCNA interactome from HDs or from G-CSF-treated donor that we have previously analyzed [15, 17, 19]. The complete list of PCNA-interactant proteins from the different assessed COVID-19 patients may be found in online supplementary Tables S3 and S4.

PCNA Is Implicated in the Response to IFNs

From the interactome findings, we raised the hypothesis that PCNA could be involved in the regulation of innate immune activation, especially through its association with key proteins of the IFN signaling pathway, as well as in the regulation of the pathogenic effector mechanisms via proteins involved in NET formation. The IFN signaling is principally regulated by STAT1 activation, including its phosphorylation, binding to specific DNA motifs in the nucleus and promoting transcription of ISGs including itself [55]. Using a PLA, we could provide evidence that PCNA can associate with p-STAT1 in response to in vitro stimulation by IFN-γ (Fig. 4c, d) and online supplementary Figure S10 for staining controls. Notably, this association was sensitive to PCNA inhibition after incubation with T2AA, a small molecule that has been shown to specifically bind and disrupt the scaffold [18] as evidenced by the quantification of the individual cell fluorescence (Fig. 4d). These data further corroborate the notion that PCNA could be a regulator of the IFN pathways through its association with p-STAT1 (Fig. 4c).

To determine the functional and biological relevance of the scaffold, we first focused on the potential role of PCNA in the IFN signaling. Therefore, we examined the mRNA expression of STAT1 and other related ISGs, such as MX1, IFIT1, and IFIT2 in ultrapure HD neutrophils treated with or without either IFN-α or IFN-γ in the presence or not of T2AA (Fig. 5a). In addition, we costimulated IFN-treated cells with TNF-α, which is present at elevated levels in the sera from COVID-19 patients and predicts in-hospital mortality in COVID-19 patients [56] and whose effects on neutrophil-derived cytokines synergize with those of IFNs [57]. We observed a strong induction of STAT1 mRNA levels in response to IFN-α, which was even potentiated by TNF-α (Fig. 5b). Interestingly, IFN-α-induced STAT1 mRNA was decreased by T2AA regardless of TNF-α stimulation. Likewise, the induction of STAT1 mRNA by IFN-γ was potentiated by TNF-α and decreased by T2AA (Fig. 5b). Consequently, mRNAs of other STAT-1-dependent genes including IFIT2 (Fig. 5c), IFIT1 (Fig. 5d), and MX1 (Fig. 5e), which were strongly induced by IFN-α, were also decreased by T2AA, suggesting that PCNA positively regulates IFN-dependent signaling pathways in neutrophils. We next tested whether PCNA modulation could also influence the release of IFN-induced cytokines (Fig. 6a), such as CXCL10 (IP-10) (Fig. 6b) and BAFF (Fig. 6c). As

3

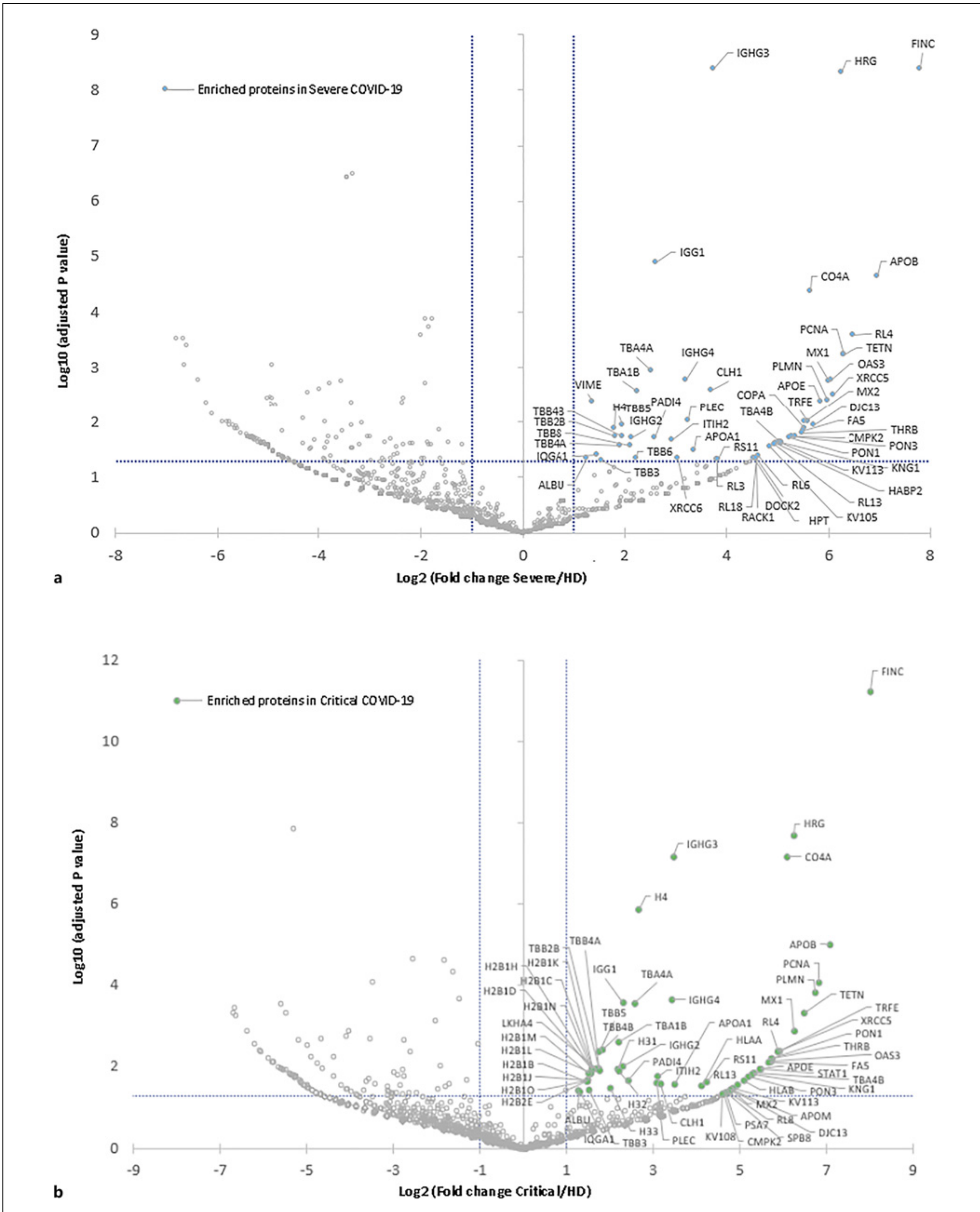

(For legend see next page.)

expected [29], CXCL10 is released in HD neutrophils treated with IFN-α and, at a higher level, with, IFN-γ, but only if cells are costimulated with TNF-α (Fig. 6b), in any case, CXCL10 production being attenuated in the presence of T2AA, significantly under IFN-γ plus TNF-α treatment (Fig. 6b). No induction of BAFF secretion was observed after stimulation with IFN-α with or without TNF-α (Fig. 6c). In contrast, we observed a remarkable induction of BAFF secretion in response to IFN-γ, which was not affected by TNF-α or by T2AA. Those results indicate the potential of PCNA in interfering with IFN-related responses and, most importantly, the use of T2AA as a pharmacological tool to blunt such effects in neutrophils.

PCNA Association with PADI4 and with Histone H3 in Neutrophils from COVID-19 Patients

We next focused our attention on the PCNA partners that are involved in the formation of NET, which has been described as one of the most deleterious mechanisms in COVID-19. According to the interactome data, PCNA interacts with PADI4 in neutrophils at different disease severity stages. Among different agonists used in research to induce NET formation, ionomycin-induced NETs has been proven to depend on PADI4 activity in neutrophils [58] but also in neutrophil-like HL-60 cell line [59]. As shown in Figure 7a, ionomycin triggers strong NET formation, as demonstrated by the release of DNA fibers containing NE and histones, whereas the same effect was barely observed in unstimulated neutrophils (Fig. 7a). Interestingly, using the Duolink PLA, we demonstrated that PCNA interacts with PADI4 in the cytosol under basal conditions, and that the proximity between the two proteins increases under ionomycin treatment (Fig.7b, c; online suppl. Fig. S11 for staining controls). Nonetheless, the association between PCNA and PADI4 was not disrupted by T2AA. In addition to PADI4, interactome analysis showed that PCNA was associated with cytosolic histone H3 only in neutrophils from critical and not from severe COVID-19. We first confirmed that the localization of histone 3 was nuclear under basal condition and became cytosolic after ionomycin treatment. Interestingly using the Duolink PLA, we observed that PCNA and histone 3 were associated within the cytosol after ionomycin treatment and this association was disrupted by T2AA (online suppl. Figs. S12, S13 for staining controls). Since histone H3 becomes citrullinated by PADI4 during NET formation, we next examined the localization of PCNA and of Cit-H3. Indirect immunofluorescence showed that, under basal condition PCNA localization was spotted with a homogeneous pattern within the cytosol and that Cit-H3 was hardly detected (Fig. 8a). In contrast, after ionomycin treatment, PCNA was redistributed into hot spots within the cytosol and seemed to colocalize with a perinuclear localization of Cit-H3. Duolink PLA was next performed to further document the interaction between PCNA and Cit-H3 (Fig. 8b; online suppl. Fig. S14 for staining controls). We observed that PCNA-Cit-H3 interaction was not observed under basal condition and was significantly increased after ionomycin treatment. Notably, this ligation was significantly decreased after T2AA treatment, thereby suggesting that the association between PCNA and Cit-H3 is located near the binding site of the T2AA molecule (Fig. 8c). Our data uncover a novel association between PCNA and both histone H3 and Cit-H3 that takes place during NET formation. Since we observed a differential effect of T2AA on the potential association of PCNA with PAD4 versus with histone 3, we examined the effect of T2AA on ionomycin-induced NET release using two different methods including (1) the isolation of NET and measurement of the DNA concentration released after 2 or 4 h of ionomycin stimulation assessed by PicoGreen (Fig. 8d) and (2) fluorescence measurement of the surface of DNA released by live imaging to study the kinetics (Fig. 8e). Whatever the readout that we used, we failed to observe any modulation of NET release by T2AA (with concentrations ranging from 10 to 50 mM) whatever the ionomycin concentration either by 4 or by 8 mM as evidenced by a representative experiment shown in Figure 8d, e. For PicoGreen assays, similar results were obtained with 4, 6, and 8 μM ionomycin for 2 or 4 h in 6 independent experiments using neutrophils isolated from different healthy individuals.

Fig. 3. Differential analysis of PCNA interactome in cytosols from patients with COVID-19 volcano plot showing proteins that interact with PCNA in neutrophils from patients with (**a**) severe COVID-19 and (**b**) critical COVID-19. Quantitative comparison of differentially expressed proteins in HD (n = 4) versus severe COVID-19 patients (n = 4) (**a**, **b**) and versus critical COVID-19 patients (n = 4) (**c**, **d**). The volcano plot represents relative protein expression changes. Blue and green dots indicate proteins upregulated in severe and in critical COVID-19 samples, respectively, with a multicomparison adjusted −log10 (p value) ≥1.3 and Log2(fold change) ≥1; gray dots indicate proteins downregulated with a multicomparison adjusted −log10 (p value) ≥1.3 and a Log2(fold change) ≤−1; gray dots also indicate proteins that do not meet either criterion. See online supplementary Tables S1 and S2 for the complete list of proteins differentially expressed in the cytosol of patients either severe or critical COVID-19 versus HD, respectively.

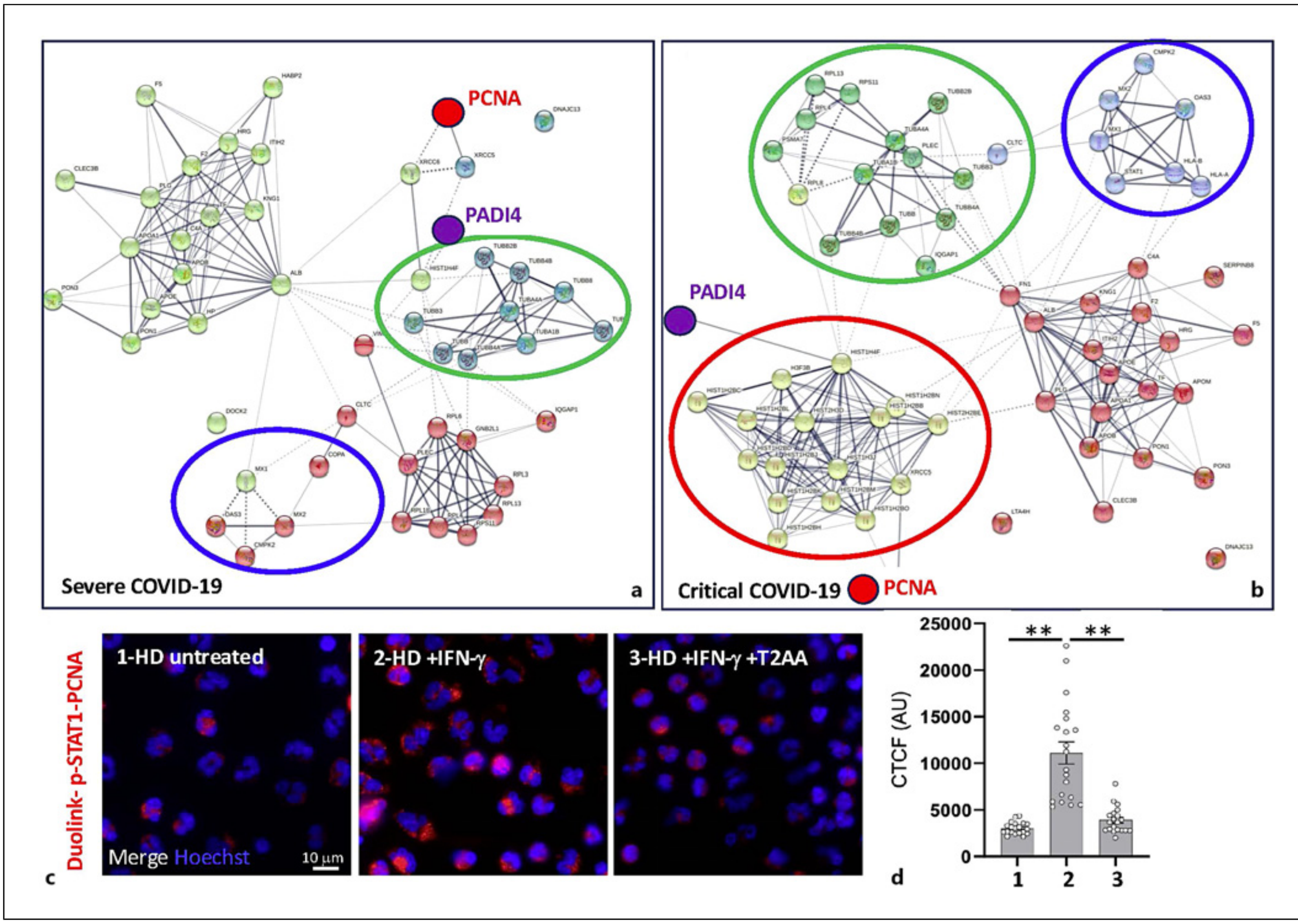

Fig. 4. Analysis of the PCNA interactome. Representation of the network of proteins that are differentially identified in the PCNA interactome in neutrophils from severe (**a**) and critical (**b**) COVID-19 patients versus HD and represented as functional clusters using the STRING online software. PCNA (red dot) has been identified in both severe and critical immunoprecipitated material. Among the common partners of PCNA between severe and critical patients are PADI4 (purple dot), the proteins involved in cytoskeleton (green circle), and IFN response (blue circle). Interaction with histone proteins has been identified only in the PCNA interactome of critical patients (red circle). See online supplementary Tables S3 and S4 for the complete list of partner proteins differentially identified in the PCNA interactome from patients either severe or critical COVID-19 versus HD. **c** Duolink proximity ligation assay of p-STAT1 and PCNA in neutrophils of HD without treatment (1) and treated with IFN-γ in the presence (3) or absence of T2AA (2). This representative experiment has been performed two times with neutrophils from two distinct HDs with similar results. **d** Quantification of the intensity of the cellular fluorescence observed in **c** was performed in samples (1-HD-untreated; 2-HD + IFN-γ; 3-HD + IFN-γ + T2AA) as described in the Materials and Methods section. Data are means of corrected fluorescence/cell ± SEM. Statistical analysis has been performed using the unpaired nonparametric Mann-Whitney test. $^{**}p < 0.01$.

Discussion

The current literature emphasizes the critical role of activated neutrophils in the pathophysiology and severity of COVID-19. However, the molecular mechanisms driving their dysregulated effector functions and sustaining their inappropriate activation remain poorly understood. Given that the cytosolic PCNA scaffold is central to the functional adaptation of neutrophils, its interactome was hypothesized to provide valuable insights into the dysregulation of these immune cells. Our study demonstrates a differential PCNA scaffold in neutrophils from COVID-19 patients compared to HDs, dominated by dysregulated metabolic pathways and a strong IFN signature.

Our findings support the notion that PCNA is involved in various neutrophil responses during SARS-CoV-2

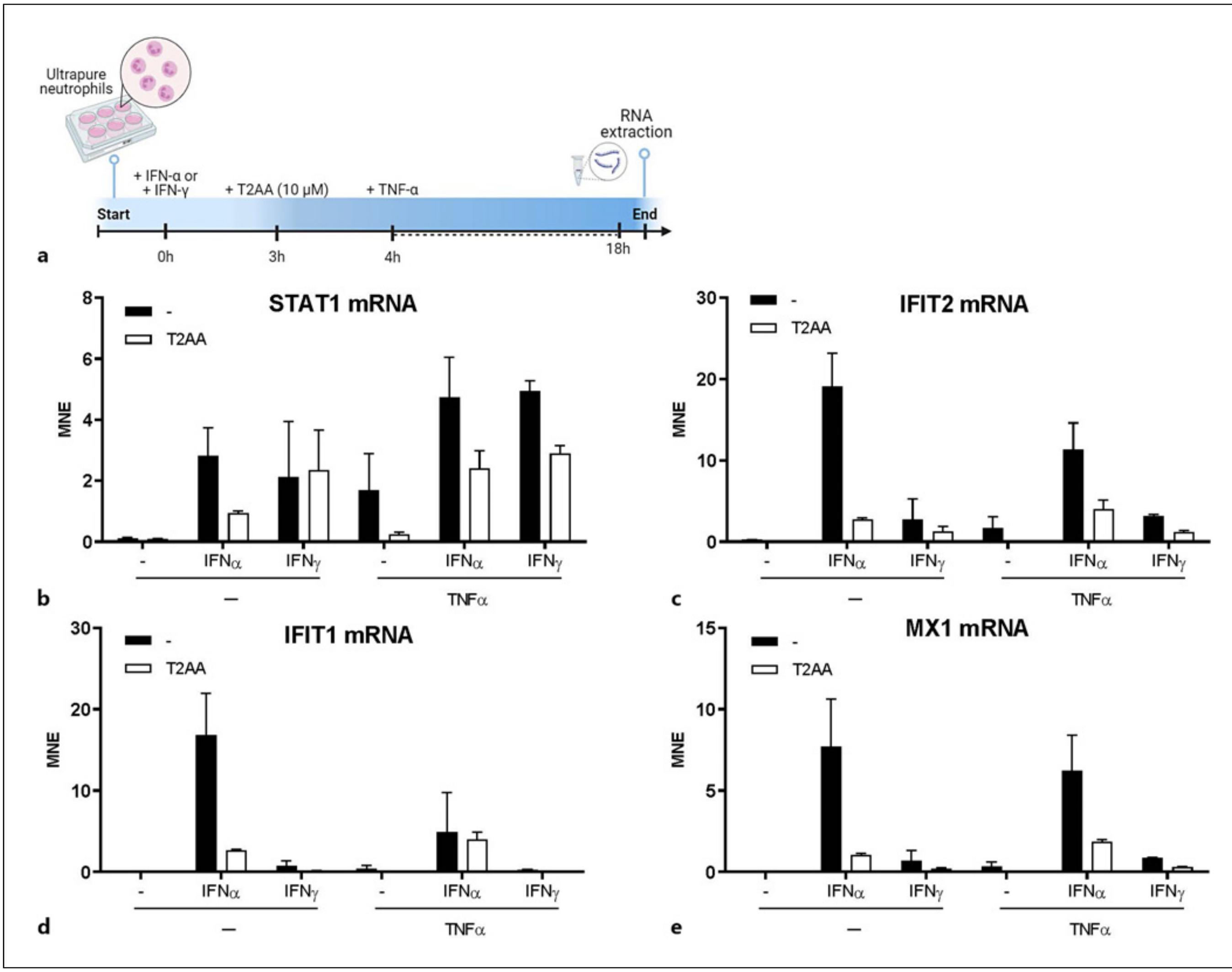

Fig. 5. Role of PCNA in regulating IFN-induced gene expression in HD neutrophils. **a** Scheme illustrating the experimental protocol used: ultrapure HD neutrophils were pretreated with 1,000 U/mL IFN-α or 200 U/mL IFN-γ, then incubated for additional 1 h with 10 μM T2AA. After 1 h, 10 ng/mL TNF-α was added and neutrophils cultured for up to 18 h. Then RNA was extracted for the assessment of STAT1 (**b**), IFIT2 (**c**), IFIT1 (**d**), and MX1 (**e**) gene expression by RT-qPCR. These experiments have been performed twice using neutrophils from two independent HDs. Data are the mean values of normalized expression (MNE) ± SEM for each condition as indicated in the Material and Methods section.

infection, acting as a hub protein that participates in IFN-mediated responses and potentially contributes to metabolic and immune dysregulation. However, whether this "maladaptive" PCNA scaffold is a driver or a consequence of the IFN-dependent disturbances observed in COVID-19 remains an open question.

From a metabolic perspective, neutrophils are unique in their reliance on nonoxidative metabolism for ATP production, even under oxygen-rich conditions [10, 60]. In the present study, we observed upregulation of glycolytic enzymes in the cytosols of patients with COVID-19 compared to HD, including a notable enrichment of triosephosphate isomerase, which catalyzes the interconversion between dihydroxyacetone phosphate and D-glyceraldehyde-3-phosphate in an early step of glycolysis. Although we did not directly measure glycolytic flux, previous studies using Seahorse technology have demonstrated significantly increased glycolysis in neutrophils from COVID-19 patients [61]. Consistently, mRNA levels of glucose transporter-1 and lactate dehydrogenase A were upregulated in COVID-19 neutrophils compared to healthy controls. This enhanced

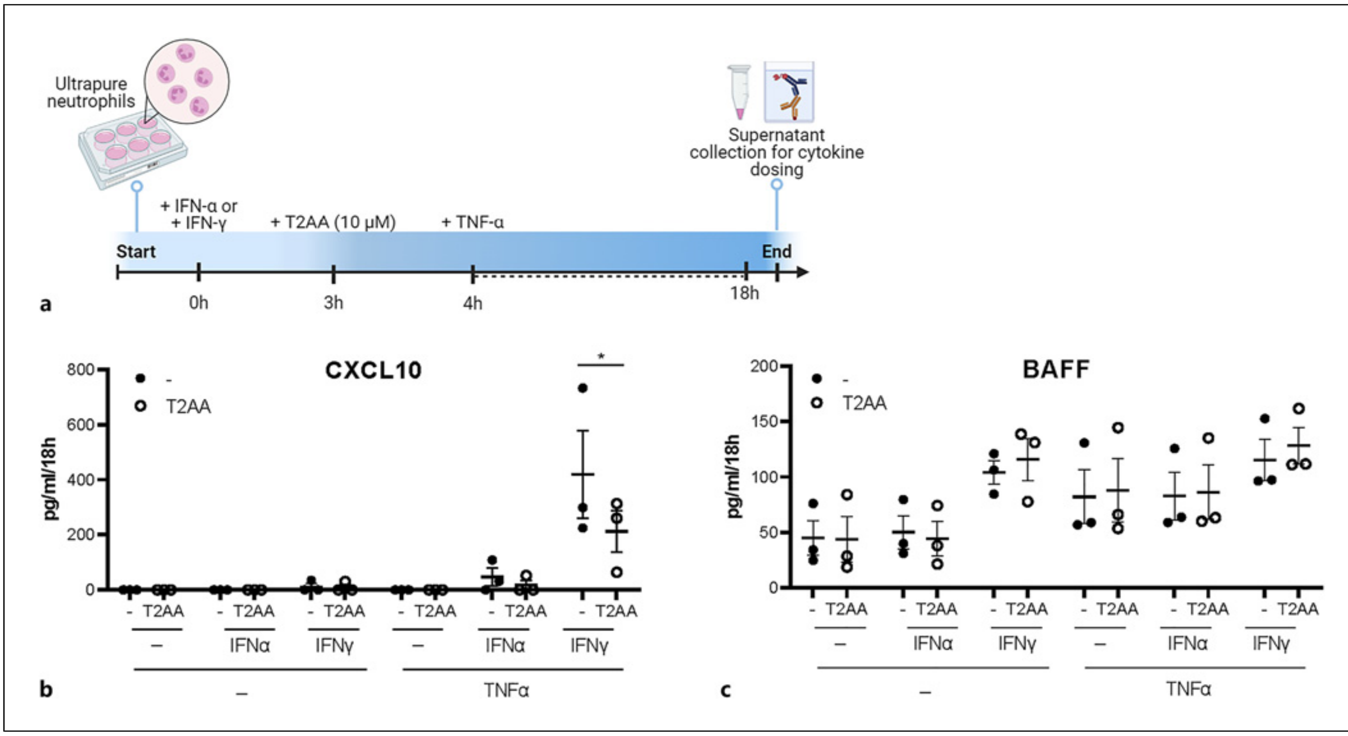

Fig. 6. Role of PCNA in regulating STAT1-dependent cytokine production by IFN-stimulated HD neutrophils. **a** Scheme illustrating the experimental protocol used: ultrapure HD neutrophils were pretreated for 3 h with 1,000 U/mL IFNα or 200 U/mL IFN-γ, before the addition of 10 μM T2AA. After 1 h, 10 ng/mL TNFα was added, and the neutrophil cultures were prolonged up to the 18-h time-point. The release of CXCL10 (**b**) and BAFF (**c**) was then assessed by ELISA in culture supernatants. Results are expressed as the mean value ± SEM of $n = 3$ independent experiments. Analysis was performed by a two-way ANOVA with Sidak's multiple-comparison test. $^{*}p < 0.05$.

glycolysis was further evidenced by increased cytosolic pyruvate kinase M2, which led to lactate accumulation and elevated plasma levels of inflammatory cytokines, including IL-1β, IL-6, IL-8, and sTNFR1 [62]. Beyond glycolysis, increased glutamate levels in COVID-19 neutrophils suggest potential gluconeogenic activity – a pathway generating glucose from noncarbohydrate substrates [45]. For instance, type I IFNs (IFN-α and IFN-β) have been shown to induce metabolic rewiring in neutrophils, favoring gluconeogenesis. In our study, we observed reduced expression of fructose-1,6-bisphosphatase 1, a key enzyme in gluconeogenesis, though we did not perform detailed metabolomic analyses to assess its impact. The regulation of glycolysis in neutrophils appears dynamic and context-dependent, varying according to the inflammatory milieu [17, 63–65]. COVID-19's inflammatory environment, characterized by a robust IFN signature, profoundly affects neutrophil metabolism. For instance, type I IFNs have been reported to inhibit glycolysis in TLR agonist-treated neutrophils [45]. In contrast, our previous work showed that G-CSF strongly enhanced glycolysis in neutrophils [17]. Accordingly, in another study, it was reported that proinflammatory cytokines combined with IFN-γ enhance glycolytic flux [61]. The observed metabolic adaptations in COVID-19 neutrophils likely represent a response to environmental stressors such as hypoxia or cytokine exposure, which might also fuel NET formation [66–68]. In parallel, a metabolomic study reported elevated pentose phosphate pathway activity and decreased GAPDH activity, potentially driving spontaneous NET formation in COVID-19 neutrophils [69]. PCNA-dependent glycolysis regulation in neutrophils differs between homeostatic and inflammatory conditions [65, 70]. Notably, we previously demonstrated that cytosolic PCNA associates with glycolytic enzymes under homeostatic conditions and inhibits glycolysis. Seahorse assays revealed that PCNA inhibitors significantly increased glycolytic capacity, highlighting PCNA's regulatory role in HD. However, during inflammation, PCNA disassociates from glycolytic enzymes, as observed in G-CSF-stimulated neutrophils, leading to enhanced glycolysis

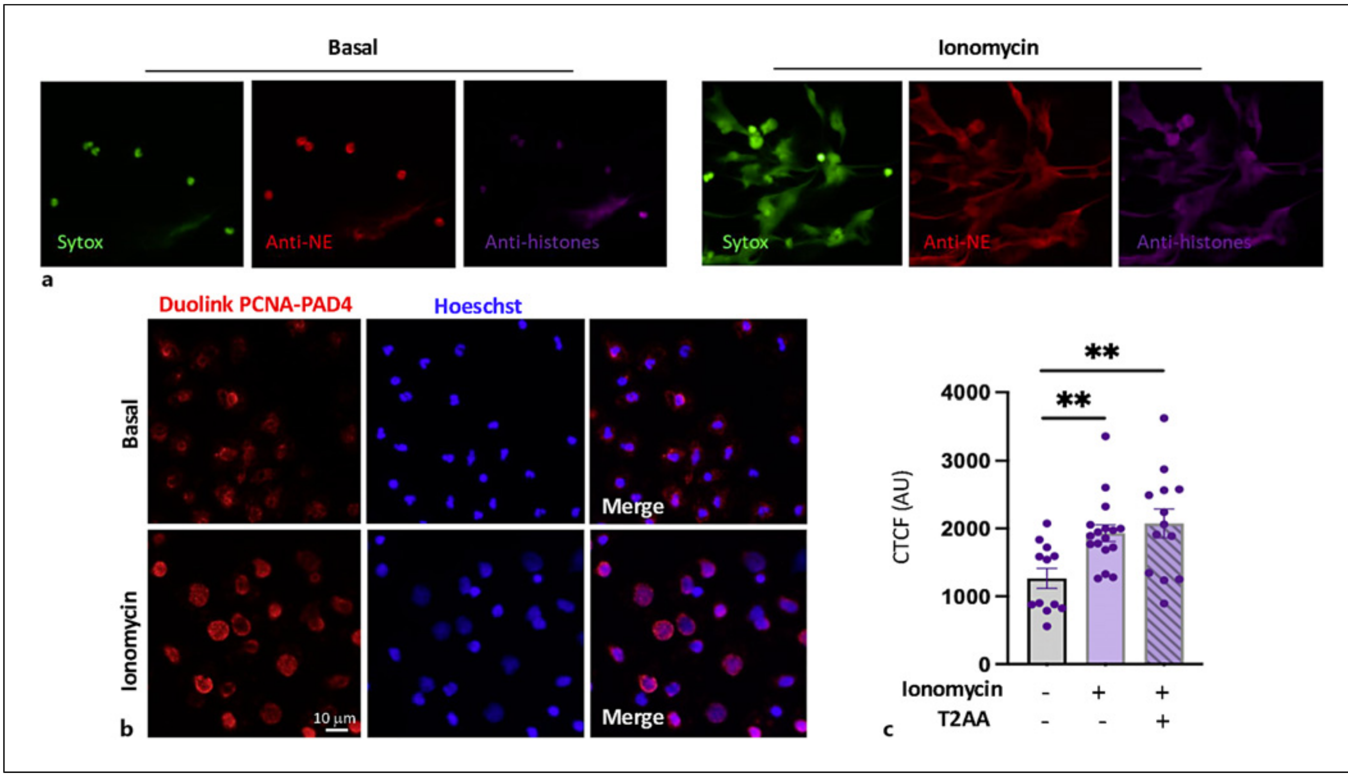

Fig. 7. Investigation of PADI4-PCNA interaction in HD neutrophils. **a** Immunofluorescence labeling of NET in resting (left panels) versus ionomycin-stimulated (right panels) HD neutrophils. NETs were stained for DNA (Sytox, green), neutrophil elastase (NE) (red), and total histones (purple). Under basal conditions, the localization of either NE or histones is intracellular, while both can be detected on extracellular DNA after ionomycin stimulation. This representative experiment has been performed two times with neutrophils from 2 different HDs with similar results. **b** Assessment of the colocalization between PCNA and PADI4 using the Duolink proximity ligation assay in basal and ionomycin-stimulated HD neutrophils in the absence or presence of T2AA (this latter condition is not shown since no effect of T2AA could be observed). This representative experiment has been performed two times with neutrophils from two distinct HDs with similar results. **c** Quantification of the intensity of the cellular fluorescence observed in **b** was performed in all the conditions (HD-basal; HD + ionomycin, HD + ionomycin + T2AA 10 μM) as described in the Materials and Methods section. Data are means of corrected fluorescence/cell ± SEM. Statistical analysis has been performed using the unpaired nonparametric Mann-Whitney test. $^{**}p < 0.01$.

independent of PCNA. Similarly, in COVID-19 neutrophils, glycolytic enzymes were absent from the PCNA interactome, suggesting that glycolysis regulation was PCNA-independent [17].

In COVID-19, the cytokine storm triggered by SARS-CoV-2 infection – characterized by elevated levels of IL-6, TNF-α, and CXCL10 – is widely regarded as a central driver of lung injury and the associated ARDS observed in severe or critical cases [71]. Our proteomic analysis reinforces this paradigm by revealing a COVID-19-specific neutrophil cytosol profile dominated by an IFN signature. This was further corroborated by the detection of cytosolic p-STAT1 in circulating neutrophils from COVID-19 patients, consistent with a phosphoproteome study identifying p-STAT1 in neutrophils during SARS-CoV-2 infection [72]. Type I IFNs are critical mediators of early innate immune responses to viral infections, acting directly to inhibit viral replication and indirectly by activating and enhancing the effector functions of immune cells [73]. Neutrophils are highly responsive to both type I and type II IFNs, cytokines known to robustly activate STAT1 [41, 74] and induce a strong expression of interferon-stimulated genes [75]. In addition, IFNs profoundly potentiate the response of human neutrophils to proinflammatory pathogen-associated molecular patterns and cytokines [40, 41, 43]. Moreover, in agreement with a role of neutrophils in the context of COVID-19, we previously showed that IFN-α potently enhances the production of IL-6 by neutrophils stimulated with TLR8 agonists, a receptor recognizing single-strand RNA of

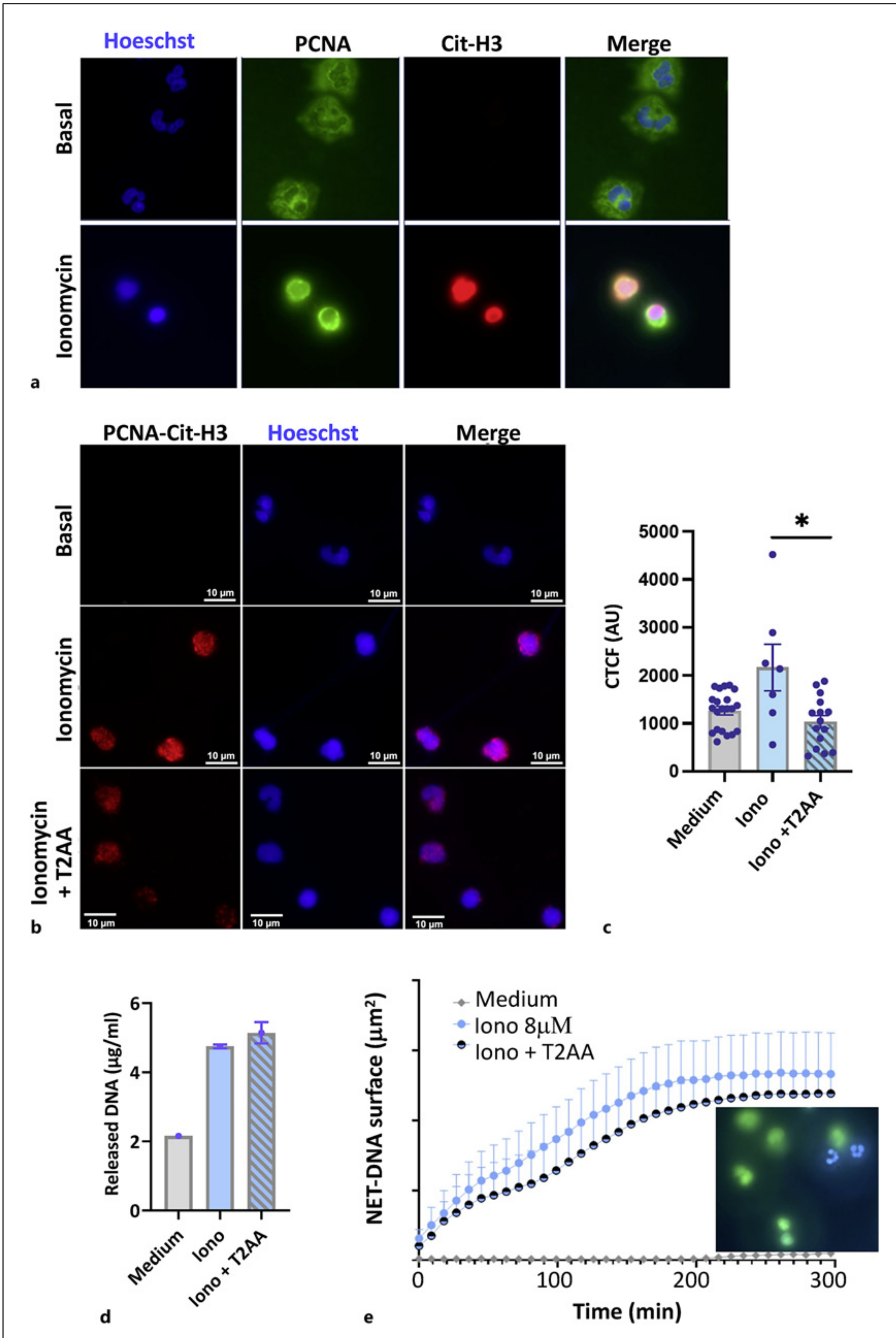

8

(For legend see next page.)

viral and bacterial origin, through an autocrine mechanism that involves an endogenous synthesis of TNF-α [41]. IFN-γ, which is also highly expressed during COVID-19, exerts immunoregulatory effects on the adaptive immune system while simultaneously enhancing the effector functions of monocytes and neutrophils [76]. For instance, both IFN-γ and IFN-α can induce the production of biologically active TNF-related apoptosis-inducing ligand [42] and CXCL10, in the latter case synergistically with TNF-α [41, 43].

CXCL10, also known as IFN-γ-induced protein 10 (IP-10), is a member of the CXC chemokine family that recruits effector cells involved in cell-mediated immunity while also exhibiting antiangiogenic properties [77]. In the context of COVID-19, CXCL10 has emerged as a robust predictive biomarker of patient outcomes, particularly for early prognosis of severe respiratory failure and mortality risk [31, 78]. Moreover, during SARS-CoV-2 infection, immature neutrophil numbers have been shown to strongly correlate with both IL-6 and CXCL10, both of which are upregulated during a cytokine storm, in association with severe ARDS [79]. As mentioned, both IL-6 and CXCL10 are two cytokines that neutrophils can produce upon IFN treatment, as also confirmed here for CXCL10. As IFN-α is produced mostly by pDC upon viral infection, together with CXCL10 upon additional TLR stimulation [80], this may indicate a potential complex interplay between pDC and neutrophils.

Our data show for the first time that in COVID-19 cytosolic PCNA can associate to phospho-STAT-1 in neutrophils, a key transcription factor that initiates both IFN-α- and IFN-γ-dependent signaling. We also show that this association is affected/dismantled by the PCNA inhibitor T2AA, concomitantly with the inhibition of STAT1, IFIT1, IFIT2, and MX1, clearly suggesting that PCNA is positively involved in the initiation of the IFN-dependent effects in neutrophils. This was further evidenced by the inhibitory effects of T2AA on CXCL10, but not BAFF production, in response to IFNs and TNF-α. This is indicative that PCNA plays a positive role specifically in the context of IFN-related interferon-stimulated gene induction.

The other insight in the COVID-19-induced PCNA scaffold is the interaction between PCNA and protein involved in NET formation including PADI4 and histone H3 [81]. PADI enzymes are calcium-dependent enzymes, which deaminate arginine residue into a citrulline [59]. PADI4 is mainly expressed in granulocytes and transferred into an enzymatic active conformation upon calcium binding. This is the reason why in vitro stimulation with the calcium ionophore (ionomycin) triggers PADI4-dependent NET formation [58]. Moreover, since PADI4 is the only PADI isoform that contains a nuclear localization sequence, it is required for nuclear histone citrullination [59]. PADI4 changes positively charged arginine to neutral citrulline on histones, thereby loosening the interaction among histones and between histones and DNA, which allows tightly packed chromatin to unravel [25, 82]. This is why citrullinated histones H3 and H4 could be considered as biomarkers for the presence of NETs in plasma and tissue sections in COVID-19 [83]. Strong correlations between NET levels and thromboinflammation have been observed in COVID-19 [28, 29, 84]. Notably, extracellular histones have been described as major mediators of death in sepsis [85] and circulating histones played a central role in COVID-19-associated coagulopathy and mortality in COVID-19 [86].

In this study, we provide evidence that T2AA has no effect on the association between cytosolic PCNA and PAD4 nor on ionomycin-induced NET release, which depends on PAD4 activity. If the PCNA-PAD4

Fig. 8. Contrasting effect of T2AA on the interaction between PCNA and Cit-H3 and on ionomycin-induced NET release in HD neutrophils. **a** Immunofluorescence labeling of PCNA and Cit-H3 in basal and ionomycin-stimulated neutrophils. This representative experiment has been performed two times with neutrophils from two distinct HDs with similar results. **b** Assessment of the colocalization between PCNA and Cit-H3 using the Duolink proximity ligation assay in basal and ionomycin-stimulated HD neutrophils in the absence or presence of T2AA. This representative experiment has been performed with neutrophils from two distinct HDs with similar results. **c** Quantification of the intensity of the cellular fluorescence observed in **b** was performed. Data are means of corrected fluorescence/cell ± SEM. *$p < 0.05$; **$p < 0.01$. **d** Measurement of released DNA after NET induction. HD neutrophils were untreated or stimulated with 8 μM ionomycin for 4 h, in the presence/absence of 25 μM T2AA, and DNA from soluble NET was quantified by fluorescence using PicoGreen. This representative experiment has been performed with neutrophils from three different HDs with similar results. **e** Live imaging of NET formation. Neutrophils were untreated or stimulated with 8 μM ionomycin in the presence/absence of 25 μM T2AA for 5 h and analyzed every 3 min. Mean and SEM of triplicates of each time point are shown. A representative picture is depicted. Nuclear DNA is stained with Hoechst 33342 (blue), while extracellular DNA is stained with Sytox green (green). This representative experiment has been performed with neutrophils from three distinct HDs with similar results.

interaction was to enhance citrullination activity and subsequently promote NET release, the lack of effect of T2AA on this interaction aligns with its inability to influence NET release, despite its inhibitory effect on the association between PCNA and Cit-H3. Interestingly, the PCNA-histone H3 association was observed exclusively in critical COVID-19 patients, suggesting that PCNA may contribute to the heightened activation of neutrophils in severe disease. However, the precise molecular mechanisms underlying this phenomenon remain unclear. While T2AA does not affect ionomycin-induced NET release, it may influence other neutrophil effector functions, such as NADPH oxidase activation, as we previously demonstrated [15, 87]. Given the potential involvement of PCNA in NET-related processes – via interactions with PAD4 and histone H3 – further research is warranted to elucidate PCNA's role in NET formation, particularly considering the diversity and complexity of these pathways in both in vitro and in vivo contexts [65, 66]. NET release can occur through multiple signaling pathways, including NOX2-independent mechanisms (e.g., ionomycin), NOX2-dependent pathways (e.g., MSU crystals, PMA, bacteria), and mitochondrial DNA-dependent processes. Additional studies are essential to clarify PCNA's role in NET release across these diverse pathways. Furthermore, we cannot exclude the possibility that T2AA might modulate NET release in response to stimuli other than ionomycin.

This study validates the concept of PCNA's versatile interactome in COVID-19 conditions and highlights its role in regulating the IFN response in neutrophils through its interaction with key proteins involved in IFN pathways, particularly p-STAT1, thereby influencing the early activation mechanisms that shape neutrophil responses [33, 46, 88, 89]. Given the wide array of proteins induced by IFN and the apparent complexity of this newly uncovered IFN-induced PCNA scaffold, further molecular studies are needed to dissect the intricate relationships between PCNA and its partners. By modulating the intensity and quality of the immune response, PCNA could play a pivotal role in shaping the adaptive immune response. Acting as a coordinator of neutrophil effector functions in response to IFNs, PCNA may ultimately determine the activation state of neutrophils, which is critical for patient outcomes in COVID-19 and presumably in other IFN-dependent immune dysregulation. Its multifaceted functions make PCNA a promising target for therapeutic interventions aimed at modulating hyperinflammation and restoring immune homeostasis in severe infections and other inflammatory diseases.

Acknowledgments

We are grateful for the excellent technical assistance provided by Christophe Rousseau and Manon Castel for the isolation of cells from COVID-19 patients, and by Julie Lesieur and Thomas Guilbert from the IMAGIC facility from the Cochin Institute. We equally thank IBEID for the support.

Statement of Ethics

Each patient with COVID-19 hospitalized at the Cochin hospital has given written informed consent according to the Declaration of Helsinki. This clinical study has been implemented by Unité de Recherche Clinique (URC) from the Cochin Hospital and has obtained ethics authorization for the patients recruited in the Department of Respiratory Medicine (University Paris Cité Ethics Committee: CPP authorization #2020 #A02700-39) and in the Department of Intensive Care Medicine (University Paris Cité Ethics Committee: CPP authorization #2018 #A01934-51). HDs were recruited from the *Etablissement Francais du Sang* and have given their written consent within an EFS-INSERM convention (AC-2020-3910) to participate to clinical research.

Conflict of Interest Statement

The authors have no conflicts of interest to declare.

Funding Sources

This study was supported by the Fondation pour la Recherche Médicale Grant EQU202003010155 (V.W.S.) and the Investissements d'Avenir programme ANR-11-IDEX-0005-02, Sorbonne Paris Cite, LabEx INFLAMEX (V.W.S.); French National Research Agency (ANR) with the Grant RA-COVID-19 V5-COVINNATE; French Government's Investissement d'Avenir program, Laboratoires d'Excellence "Integrative Biology of Emerging Infectious Diseases" ANR-10-LABX-62-IBEID (A.H.); Grant DENDRISEPSIS ANR-17-CE15-0003 (F.P.); Grant APCOD ANR-17-CE15-0003-01 (F.P.); and Lucie Pesenti was supported by LabEx INFLAMEX (3-year PhD fellowship) and Rodrigo de Oliveira Formiga had a 2-year fellowship from Campus France.

Author Contributions

All named authors meet the general criteria for the authorship of this manuscript and have given final approval for publication. V.W.S. has conceived the whole project with P.R.B. and F.P. for experiments involving neutrophils from COVID-19 patients. This includes ethic and clinical requirement and analysis, setting and conceiving in vitro and ex vivo experiments on human neutrophils, obtaining fundings, analyzing the data, and writing the manuscript. R.O.F. and L.P. have carried out experiments, analyzed data, participated to figure drawing, to manuscript writing and scientific discussions. V.W.S., R.O.F., and L.P. have presented part of the data in international scientific meetings. E.G., S.G., N.T., and M.C. conceived, performed experiments related to mRNA and ELISA analysis and have participated to the writing of the manuscript and scientific discussion; G.S.T. and F.C.d.H. performed neutrophil experiments; L.K., J.C., P.H., and M.L.G. performed the proteomic analysis; C.M. and M.Z.L. participated to the setting of the clinical study, provided the samples from COVID-19 patients, and analyzed the clinical data; P.D., M.B., and R.H. performed the NET measurements; F.C.d.H. participated in the revision of the manuscript by providing additional data of neutrophil immunolabeling and analysis of proteomic data set for supplementary figures; and A.H. participated to the setting of the clinical protocol, analyzed the data and participated to scientific discussion.

Data Availability Statement

The MS proteomics data have been deposited to the ProteomeXchange Consortium [90] via the PRIDE50 partner repository with the accession code: PXD055810 and project DOI: 10.6019/PXD055810.

References

1 Nauseef WM, Borregaard N. Neutrophils at work. Nat Immunol. 2014;15(7):602–11. https://doi.org/10.1038/ni.2921

2 Castanheira FVS, Kubes P. Neutrophils and NETs in modulating acute and chronic inflammation. Blood. 2019;133(20):2178–85. https://doi.org/10.1182/blood-2018-11-844530

3 Mantovani A, Cassatella MA, Costantini C, Jaillon S. Neutrophils in the activation and regulation of innate and adaptive immunity. Nat Rev Immunol. 2011;11(8):519–31. https://doi.org/10.1038/nri3024

4 Wright HL, Lyon M, Chapman EA, Moots RJ, Edwards SW. Rheumatoid arthritis synovial fluid neutrophils drive inflammation through production of chemokines, reactive oxygen species, and neutrophil extracellular traps. Front Immunol. 2020;11:584116. https://doi.org/10.3389/fimmu.2020.584116

5 Sugimoto MA, Sousa LP, Pinho V, Perretti M, Teixeira MM. Resolution of inflammation: what controls its onset? Front Immunol. 2016;7:160. https://doi.org/10.3389/fimmu.2016.00160

6 Jones HR, Robb CT, Perretti M, Rossi AG. The role of neutrophils in inflammation resolution. Semin Immunol. 2016;28(2):137–45. https://doi.org/10.1016/j.smim.2016.03.007

7 Chakravarti A, Rusu D, Flamand N, Borgeat P, Poubelle PE. Reprogramming of a subpopulation of human blood neutrophils by prolonged exposure to cytokines. Lab Invest. 2009;89(10):1084–99. https://doi.org/10.1038/labinvest.2009.74

8 Cassatella MA, Östberg NK, Tamassia N, Soehnlein O. Biological roles of neutrophil-derived granule proteins and cytokines. Trends Immunol. 2019;40(7):648–64. https://doi.org/10.1016/j.it.2019.05.003

9 Ganesh K, Joshi MB. Neutrophil sub-types in maintaining immune homeostasis during steady state, infections and sterile inflammation. Inflamm Res. 2023;72(6):1175–92. https://doi.org/10.1007/s00011-023-01737-9

10 Leblanc P-O, Bourgoin SG, Poubelle PE, Tessier PA, Pelletier M. Metabolic regulation of neutrophil functions in homeostasis and diseases. J Leukoc Biol. 2024:qiae025.

11 Allen L-AH. PCNA at the crossroads of human neutrophil activation, metabolism, and survival. J Leukoc Biol. 2024;115(2):201–4. https://doi.org/10.1093/jleuko/qiad153

12 Witko-Sarsat V, Ohayon D. Proliferating cell nuclear antigen in neutrophil fate. Immunol Rev. 2016;273(1):344–56. https://doi.org/10.1111/imr.12449

13 Witko-Sarsat V, Mocek J, Bouayad D, Tamassia N, Ribeil J-A, Candalh C, et al. Proliferating cell nuclear antigen acts as a cytoplasmic platform controlling human neutrophil survival. J Exp Med. 2010;207(12):2631–45. https://doi.org/10.1084/jem.20092241

14 Bouayad D, Pederzoli-Ribeil M, Mocek J, Candalh C, Arlet J-B, Hermine O, et al. Nuclear-to-cytoplasmic relocalization of the proliferating cell nuclear antigen (PCNA) during differentiation involves a chromosome region maintenance 1 (CRM1)-dependent export and is a prerequisite for PCNA antiapoptotic activity in mature neutrophils. J Biol Chem. 2012;287(40):33812–25. https://doi.org/10.1074/jbc.M112.367839

15 Ohayon D, De Chiara A, Dang PM-C, Thieblemont N, Chatfield S, Marzaioli V, et al. Cytosolic PCNA interacts with p47phox and controls NADPH oxidase NOX2 activation in neutrophils. J Exp Med. 2019;216(11):2669–87. https://doi.org/10.1084/jem.20180371

16 Inoue A, Kikuchi S, Hishiki A, Shao Y, Heath R, Evison BJ, et al. A small molecule inhibitor of monoubiquitinated Proliferating Cell Nuclear Antigen (PCNA) inhibits repair of interstrand DNA cross-link, enhances DNA double strand break, and sensitizes cancer cells to cisplatin. J Biol Chem. 2014;289(10):7109–20. https://doi.org/10.1074/jbc.M113.520429

17 Aymonnier K, Bosetta E, Leborgne NGF, Ullmer A, Le Gall M, De Chiara A, et al. G-CSF reshapes the cytosolic PCNA scaffold and modulates glycolysis in neutrophils. J Leukoc Biol. 2024;115(2):205–21. https://doi.org/10.1093/jleuko/qiad122

18 Punchihewa C, Inoue A, Hishiki A, Fujikawa Y, Connelly M, Evison B, et al. Identification of small molecule proliferating cell nuclear antigen (PCNA) inhibitor that disrupts interactions with PIP-box proteins and inhibits DNA replication. J Biol Chem. 2012;287(17):14289–300. https://doi.org/10.1074/jbc.M112.353201

19 Ohayon D, De Chiara A, Chapuis N, Candalh C, Mocek J, Ribeil J-A, et al. Cytoplasmic proliferating cell nuclear antigen connects glycolysis and cell survival in acute myeloid leukemia. Sci Rep. 2016;6:35561. https://doi.org/10.1038/srep35561

20 Leborgne NGF, Devisme C, Kozarac N, Berenguer Veiga I, Ebert N, Godel A, et al. Neutrophil proteases are protective against SARS-CoV-2 by degrading the spike protein and dampening virus-mediated inflammation. JCI Insight. 2024;9(7):e174133. https://doi.org/10.1172/jci.insight.174133

21 McKenna E, Wubben R, Isaza-Correa JM, Melo AM, Mhaonaigh AU, Conlon N, et al. Neutrophils in COVID-19: not innocent bystanders. Front Immunol. 2022;13:864387. https://doi.org/10.3389/fimmu.2022.864387

22 de Oliveira Formiga R, Amaral FC, Souza CF, Mendes DAGB, Wanderley CWS, Lorenzini CB, et al. Neuraminidase is a host-directed approach to regulate neutrophil responses in sepsis and COVID-19. Br J Pharmacol. 2023;180(11):1460–81. https://doi.org/10.1111/bph.16013

23 George PM, Reed A, Desai SR, Devaraj A, Faiez TS, Laverty S, et al. A persistent neutrophil-associated immune signature characterizes post-COVID-19 pulmonary sequelae. Sci Transl Med. 2022;14(671):eabo5795. https://doi.org/10.1126/scitranslmed.abo5795

24 Brinkmann V, Reichard U, Goosmann C, Fauler B, Uhlemann Y, Weiss DS, et al. Neutrophil extracellular traps kill bacteria. Science. 2004;303(5663):1532–5. https://doi.org/10.1126/science.1092385

25 Maronek M, Gardlik R. The citrullination-neutrophil extracellular trap Axis in chronic diseases. J Innate Immun. 2022;14(5):393–417. https://doi.org/10.1159/000522331

26 Barnes BJ, Adrover JM, Baxter-Stoltzfus A, Borczuk A, Cools-Lartigue J, Crawford JM, et al. Targeting potential drivers of COVID-19: neutrophil extracellular traps. J Exp Med. 2020;217(6):e20200652. https://doi.org/10.1084/jem.20200652
27 Veras FP, Pontelli MC, Silva CM, Toller-Kawahisa JE, de Lima M, Nascimento DC, et al. SARS-CoV-2-triggered neutrophil extracellular traps mediate COVID-19 pathology. J Exp Med. 2020;217(12):e20201129. https://doi.org/10.1084/jem.20201129
28 Middleton EA, He X-Y, Denorme F, Campbell RA, Ng D, Salvatore SP, et al. Neutrophil extracellular traps contribute to immunothrombosis in COVID-19 acute respiratory distress syndrome. Blood. 2020;136(10):1169–79. https://doi.org/10.1182/blood.2020007008
29 Ruggeri T, De Wit Y, Schärz N, van Mierlo G, Angelillo-Scherrer A, Brodard J, et al. Immunothrombosis and complement activation contribute to disease severity and adverse outcome in COVID-19. J Innate Immun. 2023;15(1):850–64. https://doi.org/10.1159/000533339
30 Radermecker C, Detrembleur N, Guiot J, Cavalier E, Henket M, d'Emal C, et al. Neutrophil extracellular traps infiltrate the lung airway, interstitial, and vascular compartments in severe COVID-19. J Exp Med. 2020;217(12):e20201012. https://doi.org/10.1084/jem.20201012
31 Samaras C, Kyriazopoulou E, Poulakou G, Reiner E, Kosmidou M, Karanika I, et al. Interferon gamma-induced protein 10 (IP-10) for the early prognosis of the risk for severe respiratory failure and death in COVID-19 pneumonia. Cytokine. 2023;162:156111. https://doi.org/10.1016/j.cyto.2022.156111
32 Arunachalam PS, Wimmers F, Mok CKP, Perera RAPM, Scott M, Hagan T, et al. Systems biological assessment of immunity to mild versus severe COVID-19 infection in humans. Science. 2020;369(6508):1210–20. https://doi.org/10.1126/science.abc6261
33 Hadjadj J, Yatim N, Barnabei L, Corneau A, Boussier J, Smith N, et al. Impaired type I interferon activity and inflammatory responses in severe COVID-19 patients. Science. 2020;369(6504):718–24. https://doi.org/10.1126/science.abc6027
34 Zhang Q, Bastard P, Liu Z, Le Pen J, Moncada-Velez M, Chen J, et al. Inborn errors of type I IFN immunity in patients with life-threatening COVID-19. Science. 2020;370(6515):eabd4570. https://doi.org/10.1126/science.abd4570
35 Galbraith MD, Kinning KT, Sullivan KD, Araya P, Smith KP, Granrath RE, et al. Specialized interferon action in COVID-19. Proc Natl Acad Sci USA. 2022;119(11):e2116730119. https://doi.org/10.1073/pnas.2116730119
36 Rosa BA, Ahmed M, Singh DK, Choreño-Parra JA, Cole J, Jiménez-Álvarez LA, et al. IFN signaling and neutrophil degranulation transcriptional signatures are induced during SARS-CoV-2 infection. Commun Biol. 2021;4(1):290–14. https://doi.org/10.1038/s42003-021-01829-4
37 Galani I-E, Rovina N, Lampropoulou V, Triantafyllia V, Manioudaki M, Pavlos E, et al. Untuned antiviral immunity in COVID-19 revealed by temporal type I/III interferon patterns and flu comparison. Nat Immunol. 2021;22(1):32–40. https://doi.org/10.1038/s41590-020-00840-x
38 Israelow B, Song E, Mao T, Lu P, Meir A, Liu F, et al. Mouse model of SARS-CoV-2 reveals inflammatory role of type I interferon signaling. J Exp Med. 2020;217(12):e20201241. https://doi.org/10.1084/jem.20201241
39 Smith N, Possémé C, Bondet V, Sugrue J, Townsend L, Charbit B, et al. Defective activation and regulation of type I interferon immunity is associated with increasing COVID-19 severity. Nat Commun. 2022;13(1):7254. https://doi.org/10.1038/s41467-022-34895-1
40 Glennon-Alty L, Moots RJ, Edwards SW, Wright HL. Type I interferon regulates cytokine-delayed neutrophil apoptosis, reactive oxygen species production and chemokine expression. Clin Exp Immunol. 2021;203(2):151–9. https://doi.org/10.1111/cei.13525
41 Zimmermann M, Arruda-Silva F, Bianchetto-Aguilera F, Finotti G, Calzetti F, Scapini P, et al. IFNα enhances the production of IL-6 by human neutrophils activated via TLR8. Sci Rep. 2016;6:19674. https://doi.org/10.1038/srep19674
42 Cassatella MA, Huber V, Calzetti F, Margotto D, Tamassia N, Peri G, et al. Interferon-activated neutrophils store a TNF-related apoptosis-inducing ligand (TRAIL/Apo-2 ligand) intracellular pool that is readily mobilizable following exposure to proinflammatory mediators. J Leukoc Biol. 2006;79(1):123–32. https://doi.org/10.1189/jlb.0805431
43 Gasperini S, Marchi M, Calzetti F, Laudanna C, Vicentini L, Olsen H, et al. Gene expression and production of the monokine induced by IFN-γ (MIG), IFN-inducible T cell α chemoattractant (I-TAC), and IFN-γ-Inducible protein-10 (IP-10) chemokines by human neutrophils. J Immunol. 1999;162(8):4928–37. https://doi.org/10.4049/jimmunol.162.8.4928
44 Schulte-Schrepping J, Reusch N, Paclik D, Baßler K, Schlickeiser S, Zhang B, et al. Severe COVID-19 is marked by a dysregulated myeloid cell compartment. Cell. 2020;182(6):1419–40.e23. https://doi.org/10.1016/j.cell.2020.08.001
45 Reyes L, A Sanchez-Garcia M, Morrison T, Howden AJM, Watts ER, Arienti S, et al. A type I IFN, prothrombotic hyperinflammatory neutrophil signature is distinct for COVID-19 ARDS. Wellcome Open Res. 2021;6:38. https://doi.org/10.12688/wellcomeopenres.16584.2
46 Long MB, Howden AJM, Keir HR, Rollings CM, Giam YH, Pembridge T, et al. Extensive acute and sustained changes to neutrophil proteomes post-SARS-CoV-2 infection. Eur Respir J. 2024;63(3):2300787. https://doi.org/10.1183/13993003.00787-2023
47 Moriceau S, Kantari C, Mocek J, Davezac N, Gabillet J, Guerrera IC, et al. Coronin-1 is associated with neutrophil survival and is cleaved during apoptosis: potential implication in neutrophils from cystic fibrosis patients. J Immunol. 2009;182(11):7254–63. https://doi.org/10.4049/jimmunol.0803312
48 Hémono M, Haller A, Chicher J, Duchêne A-M, Ngondo RP. The interactome of CLUH reveals its association to SPAG5 and its co-translational proximity to mitochondrial proteins. BMC Biol. 2022;20(1):13. https://doi.org/10.1186/s12915-021-01213-y
49 Bouyssié D, Hesse A-M, Mouton-Barbosa E, Rompais M, Macron C, Carapito C, et al. Proline: an efficient and user-friendly software suite for large-scale proteomics. Bioinformatics. 2020;36(10):3148–55. https://doi.org/10.1093/bioinformatics/btaa118
50 Kuhn L, Vincent T, Hammann P, Zuber H. Exploring protein interactome data with IPinquiry: statistical analysis and data visualization by spectral counts. Methods Mol Biol. 2023;2426:243–65. https://doi.org/10.1007/978-1-0716-1967-4_11
51 Gardiman E, Bianchetto-Aguilera F, Gasperini S, Tiberio L, Scandola M, Lotti V, et al. SARS-CoV-2-Associated ssRNAs activate human neutrophils in a TLR8-dependent fashion. Cells. 2022;11(23):3785. https://doi.org/10.3390/cells11233785
52 Ribon M, Seninet S, Mussard J, Sebbag M, Clavel C, Serre G, et al. Neutrophil extracellular traps exert both pro- and anti-inflammatory actions in rheumatoid arthritis that are modulated by C1q and LL-37. J Autoimmun. 2019;98:122–31. https://doi.org/10.1016/j.jaut.2019.01.003
53 Kaiser R, Leunig A, Pekayvaz K, Popp O, Joppich M, Polewka V, et al. Self-sustaining IL-8 loops drive a prothrombotic neutrophil phenotype in severe COVID-19. JCI Insight. 2021;6(18):e150862. https://doi.org/10.1172/jci.insight.150862
54 Romana M, Leduc M, Hermand P, Bruce J, Gautier E-F, Martino F, et al. Proteomic analysis of neutrophils from patients with COVID-19. Br J Haematol. 2022;199(1):61–4. https://doi.org/10.1111/bjh.18347
55 Wu M, Chen Y, Xia H, Wang C, Tan CY, Cai X, et al. Transcriptional and proteomic insights into the host response in fatal COVID-19 cases. Proc Natl Acad Sci USA. 2020;117(45):28336–43. https://doi.org/10.1073/pnas.2018030117
56 Smail SW, Babaei E, Amin K, Abdulahad WH. Serum IL-23, IL-10, and TNF-α predict in-hospital mortality in COVID-19 patients. Front Immunol. 2023;14:1145840. https://doi.org/10.3389/fimmu.2023.1145840

57 Cassatella MA, Gasperini S, Calzetti F, Bertagnin A, Luster AD, McDonald PP. Regulated production of the interferon-γ-inducible protein−10 (IP-10) chemokine by human neutrophils. Eur J Immunol. 1997;27(1):111–5. https://doi.org/10.1002/eji.1830270117
58 Kenny EF, Herzig A, Krüger R, Muth A, Mondal S, Thompson PR, et al. Diverse stimuli engage different neutrophil extracellular trap pathways. Elife. 2017;6:e24437. https://doi.org/10.7554/eLife.24437
59 Thiam HR, Wong SL, Qiu R, Kittisopikul M, Vahabikashi A, Goldman AE, et al. NETosis proceeds by cytoskeleton and endomembrane disassembly and PAD4-mediated chromatin decondensation and nuclear envelope rupture. Proc Natl Acad Sci USA. 2020;117(13):7326–37. https://doi.org/10.1073/pnas.1909546117
60 Morrison T, Watts ER, Sadiku P, Walmsley SR. The emerging role for metabolism in fueling neutrophilic inflammation. Immunol Rev. 2023;314(1):427–41. https://doi.org/10.1111/imr.13157
61 Borella R, De Biasi S, Paolini A, Boraldi F, Lo Tartaro D, Mattioli M, et al. Metabolic reprograming shapes neutrophil functions in severe COVID-19. Eur J Immunol. 2022;52(3):484–502. https://doi.org/10.1002/eji.202149481
62 McElvaney OJ, McEvoy NL, McElvaney OF, Carroll TP, Murphy MP, Dunlea DM, et al. Characterization of the inflammatory response to severe COVID-19 illness. Am J Respir Crit Care Med. 2020;202(6):812–21. https://doi.org/10.1164/rccm.202005-1583OC
63 Sadiku P, Willson JA, Ryan EM, Sammut D, Coelho P, Watts ER, et al. Neutrophils fuel effective immune responses through gluconeogenesis and glycogenesis. Cell Metab. 2021;33(5):1062–4. https://doi.org/10.1016/j.cmet.2021.03.018
64 Krysa SJ, Allen L-AH. Metabolic reprogramming mediates delayed apoptosis of human neutrophils infected with francisella tularensis. Front Immunol. 2022;13:836754. https://doi.org/10.3389/fimmu.2022.836754
65 Leblanc P-O, Bourgoin SG, Poubelle PE, Tessier PA, Pelletier M. Metabolic regulation of neutrophil functions in homeostasis and diseases. J Leukoc Biol. 2024;116(3):456–68. https://doi.org/10.1093/jleuko/qiae025
66 Stojkov D, Gigon L, Peng S, Lukowski R, Ruth P, Karaulov A, et al. Physiological and pathophysiological roles of metabolic pathways for NET formation and other neutrophil functions. Front Immunol. 2022;13:826515. https://doi.org/10.3389/fimmu.2022.826515
67 Amini P, Stojkov D, Felser A, Jackson CB, Courage C, Schaller A, et al. Neutrophil extracellular trap formation requires OPA1-dependent glycolytic ATP production. Nat Commun. 2018;9(1):2958. https://doi.org/10.1038/s41467-018-05387-y
68 Stojkov D, Amini P, Oberson K, Sokollik C, Duppenthaler A, Simon H-U, et al. ROS and glutathionylation balance cytoskeletal dynamics in neutrophil extracellular trap formation. J Cell Biol. 2017;216(12):4073–90. https://doi.org/10.1083/jcb.201611168
69 Li Y, Hook JS, Ding Q, Xiao X, Chung SS, Mettlen M, et al. Neutrophil metabolomics in severe COVID-19 reveal GAPDH as a suppressor of neutrophil extracellular trap formation. Nat Commun. 2023;14(1):2610. https://doi.org/10.1038/s41467-023-37567-w
70 Richer BC, Salei N, Laskay T, Seeger K. Changes in neutrophil metabolism upon activation and aging. Inflammation. 2018;41(2):710–21. https://doi.org/10.1007/s10753-017-0725-z
71 Wang J, Jiang M, Chen X, Montaner LJ. Cytokine storm and leukocyte changes in mild versus severe SARS-CoV-2 infection: review of 3939 COVID-19 patients in China and emerging pathogenesis and therapy concepts. J Leukoc Biol. 2020;108(1):17–41. https://doi.org/10.1002/jlb.3covr0520-272r
72 Turnbull IR, Fuchs A, Remy KE, Kelly MP, Frazier EP, Ghosh S, et al. Dysregulation of the leukocyte signaling landscape during acute COVID-19. PLoS One. 2022;17(4):e0264979. https://doi.org/10.1371/journal.pone.0264979
73 Trinchieri G. Type I interferon: friend or foe? J Exp Med. 2010;207(10):2053–63. https://doi.org/10.1084/jem.20101664
74 Tamassia N, Calzetti F, Ear T, Cloutier A, Gasperini S, Bazzoni F, et al. Molecular mechanisms underlying the synergistic induction of CXCL10 by LPS and IFN-gamma in human neutrophils. Eur J Immunol. 2007;37(9):2627–34. https://doi.org/10.1002/eji.200737340
75 Montaldo E, Lusito E, Bianchessi V, Caronni N, Scala S, Basso-Ricci L, et al. Cellular and transcriptional dynamics of human neutrophils at steady state and upon stress. Nat Immunol. 2022;23(10):1470–83. https://doi.org/10.1038/s41590-022-01311-1
76 Ambruso DR, Briones NJ, Baroffio AF, Murphy JR, Tran AD, Gowan K, et al. In vivo interferon-gamma induced changes in gene expression dramatically alter neutrophil phenotype. PLoS One. 2022;17(2):e0263370. https://doi.org/10.1371/journal.pone.0263370
77 Gotsch F, Romero R, Friel L, Kusanovic JP, Espinoza J, Erez O, et al. CXCL10/IP-10. J Matern Fetal Neonatal Med. 2007;20(11):777–92. https://doi.org/10.1080/14767050701483298
78 Lorè NI, De Lorenzo R, Rancoita PMV, Cugnata F, Agresti A, Benedetti F, et al. CXCL10 levels at hospital admission predict COVID-19 outcome: hierarchical assessment of 53 putative inflammatory biomarkers in an observational study. Mol Med. 2021;27(1):129. https://doi.org/10.1186/s10020-021-00390-4
79 Carissimo G, Xu W, Kwok I, Abdad MY, Chan Y-H, Fong S-W, et al. Whole blood immunophenotyping uncovers immature neutrophil-to-VD2 T-cell ratio as an early marker for severe COVID-19. Nat Commun. 2020;11(1):5243. https://doi.org/10.1038/s41467-020-19080-6
80 Decalf J, Fernandes S, Longman R, Ahloulay M, Audat F, Lefrerre F, et al. Plasmacytoid dendritic cells initiate a complex chemokine and cytokine network and are a viable drug target in chronic HCV patients. J Exp Med. 2007;204(10):2423–37. https://doi.org/10.1084/jem.20070814
81 Ackermann M, Anders H-J, Bilyy R, Bowlin GL, Daniel C, De Lorenzo R, et al. Patients with COVID-19: in the dark-NETs of neutrophils. Cell Death Differ. 2021;28(11):3125–39. https://doi.org/10.1038/s41418-021-00805-z
82 Wang Y, Li M, Stadler S, Correll S, Li P, Wang D, et al. Histone hypercitrullination mediates chromatin decondensation and neutrophil extracellular trap formation. J Cell Biol. 2009;184(2):205–13. https://doi.org/10.1083/jcb.200806072
83 Arcanjo A, Logullo J, Menezes CCB, de Souza Carvalho Giangiarulo TC, Dos Reis MC, de Castro GMM, et al. The emerging role of neutrophil extracellular traps in severe acute respiratory syndrome coronavirus 2 (COVID-19). Sci Rep. 2020;10(1):19630. https://doi.org/10.1038/s41598-020-76781-0
84 Busch MH, Timmermans SAMEG, Nagy M, Visser M, Huckriede J, Aendekerk JP, et al. Neutrophils and contact activation of coagulation as potential drivers of COVID-19. Circulation. 2020;142(18):1787–90. https://doi.org/10.1161/CIRCULATIONAHA.120.050656
85 Xu J, Zhang X, Pelayo R, Monestier M, Ammollo CT, Semeraro F, et al. Extracellular histones are major mediators of death in sepsis. Nat Med. 2009;15(11):1318–21. https://doi.org/10.1038/nm.2053
86 Shaw RJ, Abrams ST, Austin J, Taylor JM, Lane S, Dutt T, et al. Circulating histones play a central role in COVID-19-associated coagulopathy and mortality. Haematologica. 2021;106(9):2493–8. https://doi.org/10.3324/haematol.2021.278492
87 Melbouci D, Haidar Ahmad A, Decker P. Neutrophil extracellular traps (NET): not only antimicrobial but also modulators of innate and adaptive immunities in inflammatory autoimmune diseases. RMD Open. 2023;9(3):e003104. https://doi.org/10.1136/rmdopen-2023-003104
88 LaSalle TJ, Gonye ALK, Freeman SS, Kaplonek P, Gushterova I, Kays KR, et al. Longitudinal characterization of circulating neutrophils uncovers phenotypes associated with severity in hospitalized COVID-19 patients. Cell Rep Med. 2022;3(10):100779. https://doi.org/10.1016/j.xcrm.2022.100779
89 Yousefi S, Stojkov D, Germic N, Simon D, Wang X, Benarafa C, et al. Untangling "NETosis" from NETs. Eur J Immunol. 2019;49(2):221–7. https://doi.org/10.1002/eji.201747053
90 Deutsch EW, Bandeira N, Perez-Riverol Y, Sharma V, Carver JJ, Mendoza L, et al. The ProteomeXchange consortium at 10 years: 2023 update. Nucleic Acids Res. 2023;51(D1):D1539–48. https://doi.org/10.1093/nar/gkac1040